Material Matters™

Volume 6, Number 2

Rare Earths

Crucial Elements of Advanced Technologies

Gearing up for the future

Introduction

Nathan Henderson, Ph.D.
Aldrich Materials Science
Sigma-Aldrich Corporation

Welcome to the second issue of ***Material Matters*™** for 2011, *Rare Earths—Crucial Elements of Advanced Technologies*. This issue highlights the Rare Earth Elements (REE), which are essential components of modern technology and find use in numerous applications such as data storage devices, lasers, phosphors for advanced displays, catalysts, permanent magnets, and petroleum refining.[1-5] Rare Earth Elements have contributed to the digital revolution and have enabled a variety of emerging technologies, including hybrid electric vehicles and miniaturized devices and electronics.

The Rare Earth Elements are comprised of the fifteen members of the lanthanide series (lanthanum through lutetium) and yttrium. Due to similarities in chemical behavior and mineralogical occurrence, scandium is also usually included in this classification. It should be noted that the term "Rare Earth" is somewhat misleading, as these elements are not really scarce in the context of crustal abundance, especially when compared to precious metals such as gold and platinum.[6] The extraction of REEs, however, is hardly a trivial matter: these elements are rarely observed in highly concentrated, minable deposits. Furthermore, REEs are commonly found together—thus the term "fraternal fifteen" (lanthanide elements)—in rock-forming minerals, which necessitates quite sophisticated processes for separations.[7]

Sigma-Aldrich® has a long history of expertise in REE processing and offers a range of different grade materials to serve a variety of customers. In 1996, Sigma-Aldrich was identified by the U.S. Geological Survey as a key producer of high-purity scandium metal, oxide, and fluoride.[8] In the following years, however, in-house processing of REE oxides and metals has been reduced due to the broad availability of very inexpensive materials from international markets. We have recently resumed our operations to meet rising demand for REEs, which is expected to grow continuously through the next several years.[9]

The current issue of ***Material Matters*™** begins with an article by Karl Gschneidner, Jr. (Ames Laboratory, U.S. Department of Energy), who discusses the historical production of REE materials and their current shortage in the global market. In the following article, Julia Chan (Louisiana State University) describes highly correlated lanthanide intermetallics, providing an overview of material properties and a brief analysis of the molten metal flux technique used for single crystal growth. Finally, Dhanesh Chandra (University of Nevada, Reno) reviews REE-based battery materials, highlighting structures and properties of hydride-forming metal alloys as well as the role of lanthanide substitutions in optimizing their performance in nickel-metal hydride electrodes.

Each article in this issue is accompanied by a list of relevant materials available from Aldrich® Materials Science. This issue also includes a comprehensive list of REE products suitable for electronics and energy-related research. For additional product information, visit us at **Aldrich.com/matsci**. We welcome your comments, questions, new product suggestions, and custom requests (**matsci@sial.com**).

References

(1) Kane, T.J. and Byer, R.L *Optics Letters* **1985**, *10*, 65.
(2) Ronda, C.R.; Jüstel, T.; Nikol, J. *J. Alloys Compd.* **1998**, *275*, 669.
(3) Voorhoeve, R.J.H.; Remeika, J.P.; Freeland, P.E.; Matthias, B.T. *Science* **1972**, *177*, 353.
(4) Sagawa, M.; Fujimura, S.; Togawa, N.; Yamamoto, H.; Matsuura, Y. *J. Appl. Phys.* **1984**, *55*, 2083.
(5) Kitto, M.E.; Anderson, D.L.; Gordon, G.E.; Olmex, I *Environ. Sci. Technol.* **1992**, *26*, 1368.
(6) Suess, H.E. and Urey, H.C. *Rev. Mod. Phys.* **1956**, *28*, 53.
(7) Castor, S.B. and Hedrick, J.B. in *Industrial minerals & rocks-Commodities, markets, and uses*, 7th ed.; SME: Littleton, Colorado, p 769.
(8) Hedrick, J.B. *Rare Earths* U.S. Geological Survey Minerals Information **1996.**
(9) Humphries, M. *Rare Earth Elements: The Global Supply Chain* CRS Reports **2010**, R41347.

About Our Cover

Rare earth materials have been a driving force behind the digital revolution and are key components in a variety of modern electronic devices. Two examples of this are the dysprosium- and neodymium-containing magnets found in hybrid electric vehicles and neodymium- and yttrium-based materials used in lasing applications. The central motif of evolving gears represents the progression of technology fueled by the development of advanced materials.

Material Matters™
Vol. 6, No. 2

Aldrich® Materials Science
Sigma-Aldrich Corporation
6000 N. Teutonia Ave.
Milwaukee, WI 53209, USA

To Place Orders

Telephone	800-325-3010 (USA)
FAX	800-325-5052 (USA)

Customer & Technical Services

Customer Inquiries	800-325-3010
Technical Service	800-231-8327
SAFC®	800-244-1173
Custom Synthesis	800-244-1173
Flavors & Fragrances	800-227-4563
International	414-438-3850
24-Hour Emergency	414-438-3850
Website	sigma-aldrich.com
Email	aldrich@sial.com

Subscriptions

To request your **FREE** subscription to *Material Matters*, please contact us by:

Phone:	**800-325-3010 (USA)**
Mail:	**Attn: Marketing Communications** **Aldrich Chemical Co., Inc.** **Sigma-Aldrich Corporation** **P.O. Box 2988** **Milwaukee, WI 53201-2988**
Website:	**Aldrich.com/mm**
Email:	**sams-usa@sial.com**

International customers, please contact your local Sigma-Aldrich office. For worldwide contact information, please see back cover.

Material Matters is also available in PDF format on the Internet at **Aldrich.com/matsci**.

Material Matters (ISSN 1933–9631) is a publication of Aldrich Chemical Co., Inc. Aldrich is a member of the Sigma-Aldrich Group. © 2011 Sigma-Aldrich Co.

Your Materials Matter.

Jeff Thurston

Jeff Thurston, President
Aldrich Chemical Co., Inc.

Do you have a compound that you wish Aldrich® Materials Science could list to help materials research? If it is needed to accelerate your research, it matters—send your suggestion to ***matsci@sial.com*** *and we will be happy to give it careful consideration.*

Dr. Mark Allendorf of Sandia National Laboratories kindly suggested that we offer 2,2′-Diamino-4,4′-stilbenedicarboxylic acid (Aldrich Prod. No. 721247) as a linker for the synthesis of metal organic frameworks (MOFs). High surface area materials like MOFs are of interest for a variety of applications, including gas storage and sensing, catalysis, and gas separation. Stilbene derivatives have previously been used to synthesize 2- and 3-dimensional zinc-containing networks that exhibit photoluminescent behavior.[1] Stilbene-functionalized MOFs have also been used in scintillation applications for the detection of ionizing radiation.[2] The use of a functionalized linker—such as this diamino derivative—enables post-synthetic modification of an existing framework,[3] potentially allowing access to new MOF structures with unconventional properties.

References

(1) Bauer, C.A.; Timofeeva, T.V.; Settersten, T.B.; Patterson, B.D.; Liu, V.H.; Simmons, B.A.; Allendorf, M.D. *J. Am. Chem. Soc.* **2007**, *129*, 7136.
(2) Doty, F.P.; Bauer, C.A.; Skula, A.J.; Grant, P.G.; Allendorf, M.D. *Adv. Mater.* **2009**, *21*, 95.
(3) Wang, Z.; Cohen, S.M. *Chem. Soc. Rev.* **2009**, *38*, 1315.

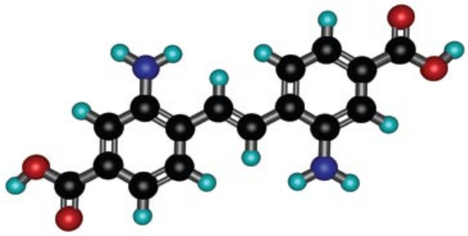

2,2′-Diamino-4,4′-stilbenedicarboxylic acid

$C_{16}H_{14}N_2O_4$ FW 298.29

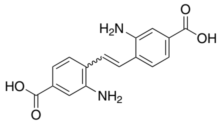

mp . . . . 200 to 205 °C

721247-500MG	500 mg

Table of Contents

Articles

Featured Products

The Rare Earth Crisis—The Supply/Demand Situation for 2010–2015

K.A. Gschneidner, Jr.
Ames Laboratory, U.S. Department of Energy and
Department of Materials Science and Engineering
Iowa State University, Ames, Iowa 50011-3020, USA
Email: cagey@ameslab.gov

Introduction

The rare earth elements impact nearly everyone in the world. All of the people living in advanced technological countries and almost all those living in third world countries utilize the rare earths in their everyday living—the car that one drives (gasoline is refined from oil using rare earth catalysts and catalytic converters reduce the polluting emissions from the automotive exhaust), watching the news on TV (the red and green colors in TV screens), the telephones and computers we use to communicate (the permanent magnets in speakers and disc drives), just to name a few examples. For a more complete listing, see **Table 1** *(on pages 34–35)*. The only way you can avoid the rare earths is to grab your sleeping bag and go into the deep forests or caves in the desert far from civilization without your cell phone or even lighter flints (which are made of iron and cerium-rich rare earths). In addition to the impact on our personal lives, the military security of the USA (and the rest of the world, likewise) is very dependent on the rare earths (permanent magnets in electric motors, computers, and guidance systems): this is also the case for our energy security (electric motors, batteries, wind turbines, petroleum refining, and fluorescent lighting). Today, 97% of the rare earths used in commerce come from mines in China (primarily the bastnäsite Bayan Obo mine, Inner Mongolia), about 2% from India, and about one-half percent or less each from Brazil, Malaysia, and the USA. This precarious situation does not bode well for the technological future of the USA and the rest of the non-Chinese world (ROW). Although the ROW can get most of the rare earths needed, the prices for Chinese-produced elements have increased by about 100% over the past year, and as much as 900% for a selected one or two rare earths—surprisingly La and Ce.

As seen in **Figure 1** the rare earth elements are reasonably abundant and lie between the 25th and 75th percentiles of natural abundance of the elements, with cerium being the most abundant rare earth and lutetium the least. The commonly mined rare earth minerals are given in **Table 2**. It is not that the rare earths are only found in China; viable deposits are known to be located in almost any corner of the world. China has about 31% of the known reserves, while the USA has one of the best minable deposits in the world—Mountain Pass, California, which is about 75 miles west of Las Vegas on Interstate 15, about 5 miles inside the California/Nevada border. If this is the situation, how did we (the ROW) get into this dilemma? And how will the ROW extract itself? Some of the answers follow in the succeeding paragraphs.

Table 2. Commonly processed ores containing rare earth elements, composition, and rare earth content (by weight). Data from USGS SIR10-5220.

Mineral	Composition	%wt REO
Monazite	$(Ce,La,Nd,Y,Th)PO_4$	35-71
Bastnäsite	$(Ce,La,Y)CO_3F$	70-74
Xenotime	YPO_4	52-67
Laterite clays	Ion-absorption clays	–
Loparite	$(Ce,Na,Ca)(Ti,Nb)O_3$	32-34

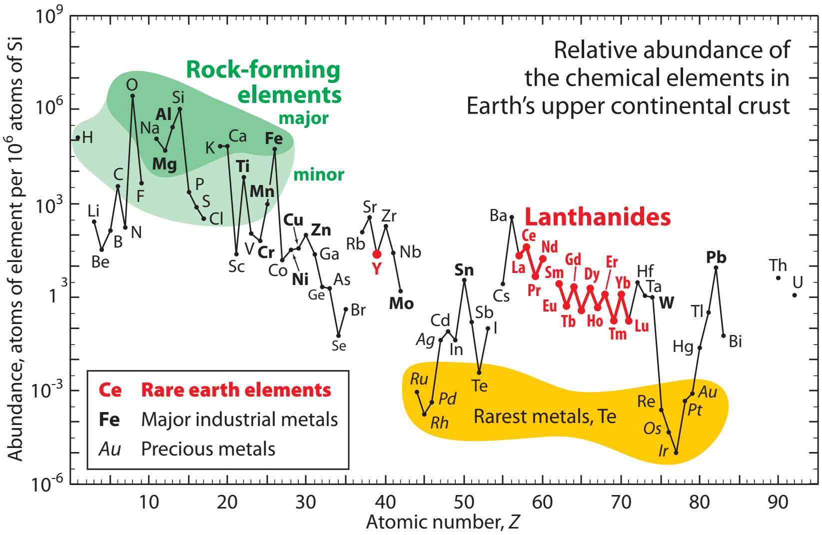

Figure 1. Relative abundance of rare earths (highlighted in red). Figure courtesy of Gordon Haxel, USGS.

History

The production of the rare earths was ~2 ktons per annum before 1960, and it grew at a rate of about 10% per year, up to 124 ktons in 2010. The discovery of the intense red luminescence of Eu when excited by electrons, which was quickly utilized in color TV in the early 1960s, was the start of the growth process of the rare earth industry. Production of rare earth oxides from Molycorp's Mountain Pass, California bastnäsite deposit started in 1964, and within two years the company supplied 50% of the rare earth oxides consumed in the world, continuing to do so until 1984. In 1985, China began to export mixed rare earth concentrates, and by 1990, its production exceeded that produced in the USA. In the early 1990s, China began to export separated rare earth oxides and metals, and reduced the amount of mixed rare earths supplied to the rest of the world. By the late 1990s, the Chinese continued to move up the supply chain to higher value products such as magnets, phosphors, and polishing compounds. Since the turn of the century, China has supplied finished products including electric motors, computers, batteries, liquid crystal displays (LCDs), mobile phones, and portable music devices. More details concerning these changes can be found in recent articles published in *Science*,[1] *Chemical and Engineering News*,[2] and *Bloomberg/Business Week*.[3]

In 1970, China had 75% of the known rare earth reserves and, based on this, started to demonstrate a strong presence in the rare earth markets. However, in the subsequent 30 years, the percentage of Chinese reserves dropped to about 30% because of the discovery of new deposits all over the world, even though the absolute amount of the known Chinese reserves grew by about 290%. Recently, China has changed its approach to the rare earth market, and they have introduced production quotas, export quotas and export taxes, enforced environmental legislation, and granted no new rare earth mining licenses. Furthermore, China has stated that they will no longer export rare earth-finished products, because of rapid growth of internal markets and limited reserves, especially the heavy rare earths (Gd through Lu). As a result, the price for rare earth materials and products containing rare earths has risen to a level at which the ROW mining companies and producers can be competitive and make a profit. The non-Chinese production of rare earth oxides (REO) per year was estimated to be 4 ktons in 2009. There is another important source of rare earth materials: those that are smuggled out of China; most of which are the highly valued heavy lanthanides and yttrium coming from South China's xenotime and laterite clays deposits. The black market was estimated to be 30-40 ktons in 2007, i.e., about 20% of the officially published numbers. Naturally, the Chinese government is trying to stop this leakage, and they seem to be successful since the latest estimate decreased to about 15-20 ktons in 2010.

The various applications for the mixed and the individual rare earths are presented in the fourth column of **Table 1**. Also listed are the estimated current demand (column 3) and the percentage of a given rare earth commodity relative to the entire market (column 2 and **Figure 2**). The market situation for each rare earth—balanced, surplus, tight (shortage)—is also noted in **Table 1** (column 3). The largest markets are Ce (30% of the total by weight), mixed rare earths (28%), La (25%), Nd (16%) and Pr (5%). Of the ten remaining other markets, three are 2% or less (Sm, Gd and Dy), and the other seven account for less than a half of a percent each. It is noted that only about 43% of the cerium mined today is utilized, and if it were completely utilized cerium's share of the market would be nearly 50%. Even though cerium is relatively inexpensive to separate compared to the other rare earths—a simple oxidation/reduction process—it must be first removed from the flow stream in order to begin the processing of the other rare earths by a counter current liquid/liquid extraction process.

There is also a second penalty: it must be stored (about 50 kton per year). The rare earth industry would greatly welcome new, large (tens of ktons) cerium applications. If the cerium market were balanced, it would significantly reduce the costs of the other rare earth elements. The rare earth usage by various applications is shown in **Figure 3**. Shown in **Figure 4** are some high purity (research grade) rare earth metal, oxide, and fluoride samples produced at the Ames Laboratory's Materials Preparation Center.[4]

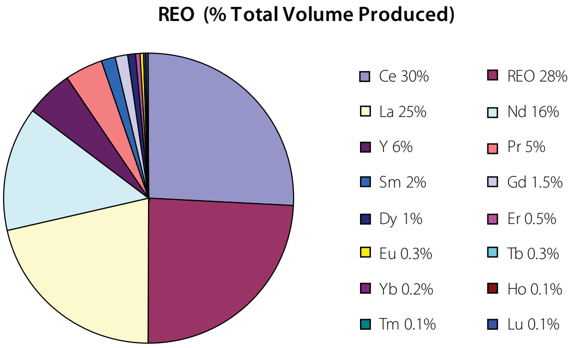

Figure 2. Distribution of rare earths by percentage of total volume produced. REO reflects mixed metal rare earth oxides.

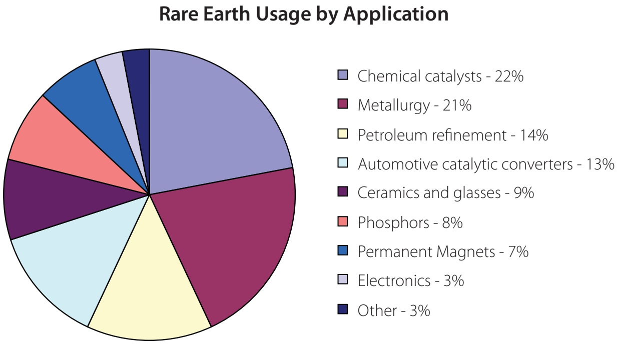

Figure 3. End use distribution of rare earth elements by application in 2009. Data from USGS Mineral Commodity Summaries.

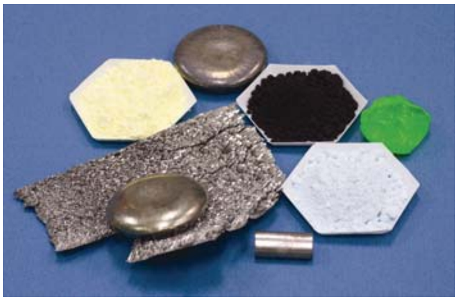

Figure 4. Rare earth metals (arc-melted buttons and a cast rod), oxides (powders), and fluorides (crystals). Source: Ames Laboratory

Table 1. Uses and Markets of the Rare Earth Elements

RE Element	% of Total Volume of REO Produced	Current Demand	Uses
Mixed Rare Earth Oxides REO	28	Balanced; 40 kton REO	**Petroleum cracking catalyst** **Mischmetal** steels (refining) **ductile iron** **lighter flints** alloying agent – Mg, Al, cast iron **Ni metal hydride batteries** **Polishing compounds** Condensers, $BaTiO_3$ Fertilizers
Lanthanum La	25	Balanced; 36 kton REO	**Nickel metal hydride batteries (Prius, forklifts)** Hydrogen storage alloys $LaNi_5$ Alloying agent – Mg, Al, cast iron, superalloys Sputtering targets **Optical** lenses (increase index of refraction) Host for phosphors fluorescent lamps X-ray intensifying screens **Petroleum cracking catalyst** Condensers, $BaTiO_3$ Heavy metal fluoride glasses fiber optics Night vision goggles
Cerium Ce	30	Surplus; 42 kton REO (supply 55 kton REO)	**Catalysts** **automotive 3-way emission catalysts** **petroleum cracking** water purification Glass additives decolorizer **UV light absorption (protection of contents from deterioration)** **Polishing media** glass, lenses, face plates of monitors semiconductors Ce-stabilized ZrO_2 structural ceramics synthetic gems (pale yellow) Phosphors fluorescent lamps scintillation counters Condensers, $BaTiO_3$ Alloying agent – Mg, Al, cast iron, superalloys Steels (refining) Sputtering targets
Praseodymium Pr	5	Balanced; 7 kton REO	**Additive to $Nd_2Fe_{14}B$ (reduces amount of Nd used)** Pr-stabilized ZrO_2 (synthetic gems – light green) Coloring agents glass – light green ceramic tile – yellow Condensers, $BaTiO_3$ Scintillators for x-ray tomography Glass blower's and welder's goggles (with Nd)
Neodymium Nd	16	Tight (slight shortage); 23 kton REO; 2.8 kton Nd metal for wind turbines (USA)	**$Nd_2Fe_{14}B$ permanent magnets** **electric motors (largest), spindles for computer hard drives (second largest), cell phones, iPods®, direct drive, wind turbines, actuators** Alloying agent for Mg alloys Lasers glass, YAG (yttrium aluminum garnet) Metal halide lamps Nd-stabilized ZrO_2 synthetic gems (pink/purple) Coloring agent glass (pink to purple) Condensers, $BaTiO_3$ Glass blower's and welder's goggles (with Pr)
Samarium Sm	2	Balanced; 2.8 kton REO	**SmCox permanent magnets ($5 \le x \le 8.5$) for above room temperature applications** Coloring agent glass (light yellow) Phosphors monitors, TV screens
Europium Eu	0.3	Balanced; 0.4 kton REO	**Phosphors (red color)** **TVs** **fluorescent lamps (CFL and LFL)** scintillators for x-ray tomography Phosphors (blue color) LEDs

RE Element	% of Total Volume of REO Produced	Current Demand	Uses
Gadolinium Gd	1.5	Balanced; 2.1 kton REO	**Host for phosphors** **fluorescent lamps** **scintillators for x-ray tomography** **MRI contrast agents** Nuclear – poison, safety **X-ray intensifying screen** YGG (yttrium gadolinium garnet) communications (radio frequencies) phase shifters, tuners, filters, radar Optical lenses
Terbium Tb	0.3	Tight (shortage); 0.4 kton REO	**Phosphors (green color)** **fluorescent lamps (CFL and LFL)** **monitors and TV screens** **LEDs** X-ray intensifying screens **Teferol-D ($(Tb_{0.3}Dy_{0.7})Fe_2$** **magnetostrictive alloy** Magneto-optic disks
Dysprosium Dy	1.0	Tight (shortage); 1.4 kton REO	**Additive to $Nd_2Fe_{14}B$ permanent magnets to improve high temperature performance, increase coercivity** Phosphors Metal halide lamps Teferol-D ($(Tb_{0.3}Dy_{0.7})Fe_2$ magnetostrictive alloy
Holmium Ho	0.1	Surplus; 0.1 kton REO	Research Metal halide lamps
Erbium Er	0.5	Balanced; 0.7 kton REO	**Fiber optics** **signal amplifiers** Lasers Coloring agent (pink) Er-stabilized ZrO_2 – synthetic gems (pink)
Thulium Tm	0.1	Surplus; 0.1 kton REO	X-ray intensifying screens Metal halide lamps Research
Ytterbium Yb	0.2	Surplus; 0.3 kton REO	Optical lenses (Yb^{2+}) Pressure sensors (metal) Research
Lutetium Lu	0.1	Surplus; 0.1 kton REO	Research Host for scintillator detectors and X-ray phosphors Optical lenses
Yttrium Y	6	Balanced; 8.5 kton REO	**Host for phosphors** **fluorescent lamps (CFL and LFL)** **monitors and TV and LCD screens** **YAG (yttrium aluminum garnet)** **laser host material** **Y-stabilized ZrO_2** **electronic (oxygen sensor; automobiles)** **structural (tough ceramics)** synthetic gems (simulated diamonds) **thermal barrier coatings (turbines, aircraft engines)** YGG (yttrium gadolinium garnet) communications (radio frequencies) phase shifters, tuners, filters, radar **YIG (yttrium iron garnet)** **communication (radio frequencies)** **radars, phase shifters, filters** YBa_2CuO_7 high temperature superconductor power transmission lines magnets for wind turbines SiN ceramics – sintering aid (Y_2O_3) Optical lenses Alloying agent for superalloys – corrosion & oxidation resistant Mg (high temperature creep resistance)

(REO = rare earth oxide equivalent)
Most important uses are in bold

Future

Mining

The best forecast suggests that ROW mining companies need to increase their output of 6 ktons in 2010 to 50 ktons in 2015 to meet the growing demand. It is anticipated that the Mountain Pass mine will be in full production in 2012, supplying 20 kton/year and doubling that amount in the second phase of their expansion in 2013. The Mount Weld monazite mine in Australia will start production in 2011 and will be able to supply 21 kton/year in 2013. These two companies should be able to make up most of the projected demand through 2014-2015. These two deposits, however, contain predominantly the light rare earth elements (La, Ce, Pr, Nd and Sm). The demand for Nd and the heavy rare earths Tb and Dy will be tight for the 2011-2015 semi-decade. There are a number of smaller deposits with a large fraction of these three elements, which are expected to come on stream in the 2014-2015 time frame, potentially easing the pressure for the heavy rare earth elements.

The two important non-Chinese mines in operation today are the Orissa placer deposit (Toyota, India) and the bastnäsite Dong Pao mine (co-owned by several Asian companies, Vietnam). Both are producers of the light lanthanides and account for about 5 kton REO from the ROW. Five additional light lanthanide rare earth mines are anticipated to become operational in the 2013-2015 period. In addition to these ten sources, there are between 100 to 150 deposits that have been promoted as possible rare earth sources, but most will never become fully functioning mines. If most of the promising new mines and the established ones come on stream, there will be an excess of rare earth oxides in the market in the 2015-2020 time frame, assuming the demand increases by 10% per year.

Mid-supply Chain and Original Equipment Manufacturers

Although it appears that the mined ores, the processed rare earth concentrates, and the separated individual rare earths should meet the 2011-2015 demand for these starting materials, the major problem will be absence of ROW manufacturers in the supply chain to convert the rare earth oxides into useful products, e.g., magnets, batteries, phosphors. This also applies to the ROW original equipment manufacturers (OEM) of the final products [such as computers, electric motors, cell phones, compact fluorescent lamps (CFL), LCDs, and batteries] since they were driven out of business in the 1990s. It does not make much sense to mine and process the rare earth starting materials in the U.S. and send them to Asia for final product production before shipping them back to the United States.

The U.S. and ROW governments need to take vigorous action to re-establish mid-supply chain and OEM industries which can effectively compete on a global scale. The most direct way to invigorate the mid-supply chain and OEMs is to establish long-term guaranteed loans to these organizations to convert the mined rare earth oxides to metals for magnets, batteries, and magnetic refrigeration systems, and to other useful compounds for phosphors, optical components, catalysts, etc. These companies need to modernize, using the latest available technologies and automate the production processes—this is the only way we will be able to effectively compete on a global scale.

Training Scientific and Engineering Personpower

The lack of trained and experienced scientists and engineers, especially those younger than 50 years old, to fill in these technological gaps in the supply chain also contributes to the ROW's dilemma. Many of the older living scientists and engineers who were working for firms in the rare earth supply train have either retired or moved on to new positions and are not likely to come back into the rare earth industry. The lack of an intellectual infrastructure can be addressed by establishing a National Research Center for Rare Earths at an educational institution with affiliations with other universities, colleges and research centers. This was recently discussed in more detail by the author.[5]

Upon completion of their studies, the students will enter the workforce, i.e., industry, educational institutions, government, non-profit laboratories, etc. There is another five to ten years on the average before they reach their full potential. This is the point, and beyond, where they invent new products, design new and improved processes to make the new and the old mature devices and products more economical (and perhaps simultaneously by environmentally green technologies), become our future educational leaders, and make other scientific and technological contributions to society. These are the persons who will help regain our technological leadership and inventiveness that we once had in the 1980s and early 1990s. Thus, the Center's mission should be completed in a 10-to-15-year framework from the date it starts—a long time, but a big pay off. This is a chance the U.S. and ROW need to take.

Other Solutions

At the present time, there is little to no recycling of rare earth-containing products, except in Japan, but some research efforts have been started, at least in the U.S. It is likely that more research on this topic will be funded by the ROW national governments. One of the major problems is that although the rare earths are essential components of electronic devices, etc., they only constitute a small fraction of weight/volume of the final product (e.g., a computer). As a result, the percentage is about the same as that of the poorer ore bodies (i.e., ~2%) which are mined today. For cell phones and portable music devices it is much worse, the rare earth magnets weigh less than 0.1% of the device.

Currently, there is a small effort to find substitutes for the rare earth elements, but this is a difficult task due in part to their unique electronic structure and the unique properties of the 4*f* electron orbitals. The major high technological applications (optics, phosphors, fluorescent lighting, electronic devices, magnets) of the rare earth (lanthanide)-based materials depend upon the specific 4*f* electron configuration of each element. Therefore, the applications are quite unique, making it difficult to find other elements to substitute for the rare earth atom, even one lanthanide for another. The odds of finding a substitute for a particular rare earth range from slim to none depending on the application. Scientists and engineers have been looking for substitutes from day one when the new application became viable. For example, the red color in TVs is due to Eu—it has been around for over 50 years and no substitute has been found; likewise, over 30 years have passed for the Sm permanent magnets (Aldrich Prod. Nos. 692859, 692840, 692832) and the 3-way Ce automotive catalytic converter, and about 27 years for the Nd-Fe-B (Aldrich Prod. Nos. 693790, 693782, 693820) permanent magnets, and still no viable substitutes demonstrating identical performances have been found. It is not that we should not try, but we must realize that success is not very likely.

However, partial substitution of one lanthanide by another may extend the utilization of the parent lanthanide. For example, partial substitution of Pr for Nd in the Nd-Fe-B permanent magnets is possible, but since there are about 4 Nd atoms per 1 Pr atom in the original ore source, this merely reduces the amount of Nd used in these permanent magnets, but it has the additional advantage in that Pr is not a by-product which must be stored. Another situation is the replacement or partial substitution of La in the nickel metal hydride (Aldrich Prod. No. 685933) battery by mischmetal (a metallic mixture of the naturally occurring rare earth ore—50% Ce, 25% La, 15% Nd, 4% Pr). In both cases there is some reduction of the performance of the magnet or the battery, but the properties are still sufficient for some applications.

There is one possible viable substitution of the rare earth permanent magnets in direct drive wind turbines and that is to use the high temperature ceramic $YBa_2Cu_3O_7$ (Aldrich Prod. No. 328626) superconductor operating at ~50 K to generate the magnetic field.[6] This, however, trades one rare earth (Y) for another (Nd), and this would put pressure on the Y market, which is currently in balance, to relieve the pressure in the Nd market. Is this a good trade-off?

One can always go back to the product that the rare earth replaced and use it instead. But would the user accept the inferior performance? For example, laptop computers would be about 50% bigger in size and weigh twice as much. Similarly, the automotive industry would have to return to heavier and bulkier electric motors, and as a result, reduce the mileage one gets from a gallon (liter) of gasoline—this is not likely, since automotive companies are striving very hard to meet government CAFE (corporate average fuel economy) standards (35.5 miles per gallon in 2016) to increase the number of miles one gets from a gallon of fuel.

There is a great deal of uncertainty about the future rare earth markets because of the size of China's market share of rare earth supplies and refining. Additionally, China claims that in a few years (by 2015) they will no longer supply any rare earth materials to the ROW because they expect their internal rare earth consumption will utilize all of the domestically mined rare earths. The question is, will they begin to import some rare earths, primarily the heavy lanthanides plus yttrium after 2015? Or will they increase their internal production? The former is the most likely scenario because Chinese mining companies are actively trying to buy major ownership in global rare earth ore sources, especially those that have a predominance of yttrium and heavy lanthanides. This is because their ion absorption (laterite) clay deposits are expected to be depleted by 2025 or earlier. This leaves them with only one known xenotime deposit in Guangdong as their primary source of heavy rare earths.

China appears to be continuing to control their share of the rare earth market at the mining, beneficiation, and initial separation stages (i.e., they are no longer exporting these commodities). Using these materials internally directly affects the supply of rare earth products further up the supply chain, where the ROW is the weakest due to the demise of the technical, scientific, and entrepreneurial rare earth infrastructure, which deteriorated in the late 1990s and early 2000s.[5]

It is extremely unlikely that Chinese producers will lower their prices of the entire rare earth market as they did initially to establish a strong market presence (roughly 1992-2005). They may, however, lower prices on selected rare earths for some economic advantages. Regardless, the ROW can meet the growing demand for rare earth materials by re-establishing mining, processing, and refinement capabilities; developing the mid-supply chain and production of finished products; and training the next generation of scientists to contribute to the rare earth industry.

Acknowledgments

The author thanks his colleagues V.K. Pecharsky, A.H. King, I.E. Anderson and S.R. Karsjen, and Nathaniel Henderson, Sigma-Aldrich, for their constructive comments. Work at Ames Laboratory is supported by the Office of Basic Energy Sciences, Materials Sciences Division of the Office of Science of the U.S. Department of Energy under Contract No. DE-AC02-07CH11358 with Iowa State University.

References

(1) Stone, R. *Science* **2009**, *325*, 1336.
(2) Jacoby, M.; Jiang, J. *Chem. Eng. News* **2010**, *88*, 9.
(3) Robison, P.; Ratnam, G. Pentagon Losing Control of Bombs to China's Monopoly. *Bloomberg/Business Week*, Sept. 30, 2010.
(4) Materials Preparation Center, The Ames Laboratory, U.S. Department of Energy. Ames, IA, USA. http://www.mpc.ameslab.gov (accessed April 2011).
(5) Gschneidner, K.A., Jr. *Magnetics Business & Technology* **2011**, *10(1)*, 6.
(6) American Superconductor, Sea Titan Data Sheet, http://www.amsc.com/products/applications/windenergy/seatitan.html (accessed April 2011).

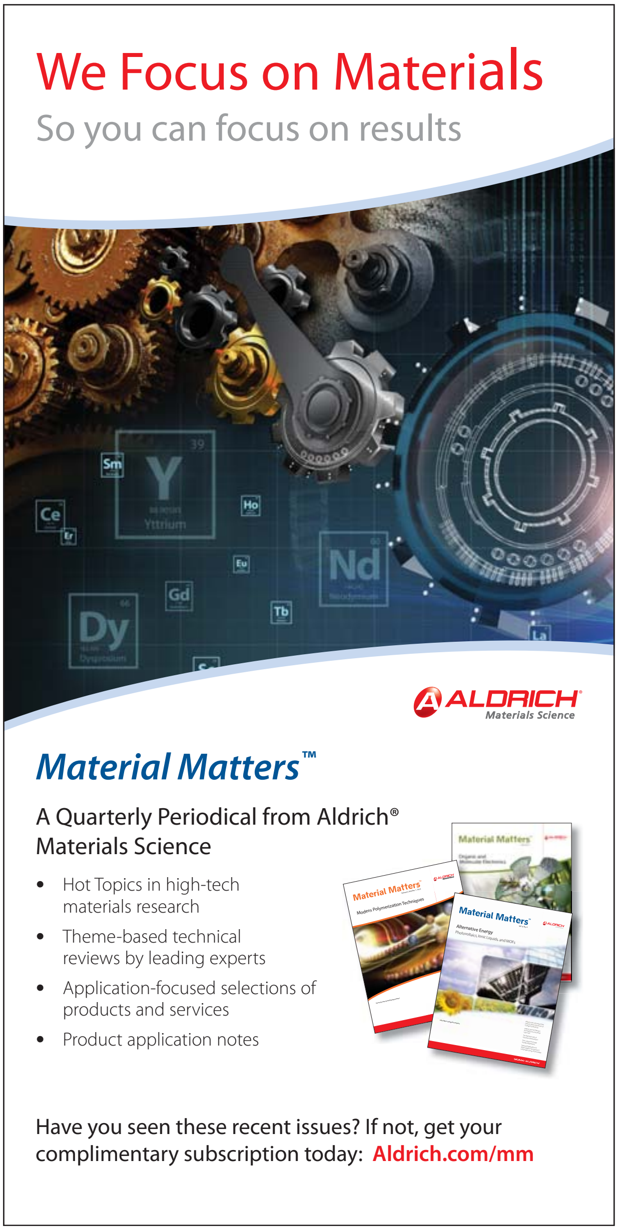

Rare Earth Metal Salts

For a complete list of available salts, visit Aldrich.com/metalsalts

Rare Earth Halides

Name	Formula	Purity	Physical Form	Prod. No.
Cerium(III) bromide	$CeBr_3$	99.9% trace metals basis	powder	449725-1G
Cerium(III) chloride	$CeCl_3 \cdot 7H_2O$	99.999% trace metals basis	crystals and lumps	202983-10G 202983-100G
Cerium(III) chloride	$CeCl_3 \cdot 7H_2O$	99.9% trace metals basis	crystals and lumps	228931-25G 228931-100G 228931-500G
Cerium(III) fluoride	CeF_3	99.99% trace metals basis	powder	229555-2G 229555-10G 229555-50G
Cerium(IV) fluoride	CeF_4	99%	powder	435937-5G
Cerium(III) iodide	CeI_3	≥99.95%	powder	456829-1G
Dysprosium(III) bromide	$DyBr_3$	99.99% trace metals basis	powder	429376-1G 429376-5G
Dysprosium(III) bromide	$DyBr_3 \cdot xH_2O$	99.999% trace metals basis	solid	575240-5G 575240-25G
Dysprosium(III) chloride	$DyCl_3$	99.99% trace metals basis	powder	325546-5G 325546-25G
Dysprosium(III) chloride	$DyCl_3 \cdot 6(H_2O)$	≥99.99% trace metals basis	solid	203173-10G
Dysprosium(III) chloride	$DyCl_3 \cdot 6(H_2O)$	99.9% trace metals basis	crystals and lumps	289272-25G 289272-100G
Dysprosium(III) fluoride	DyF_3	99.99% trace metals basis	powder	450847-25G
Dysprosium(III) fluoride	DyF_3	99.9%	solid	372587-25G
Dysprosium(II) iodide	DyI_2	≥99.9% trace metals basis	powder	652423-1G
Dysprosium(III) iodide	DyI_3	99.99% trace metals basis	flakes	429333-1G 429333-5G
Erbium(III) bromide	$ErBr_3{\cdot}xH_2O$	99.999% trace metals basis	solid	575224-25G
Erbium(III) chloride	$ErCl_3$	99.9% trace metals basis	powder	449792-5G 449792-25G
Erbium(III) chloride	$ErCl_3{\cdot}6H_2O$	99.995% trace metals basis	solid	203211-20G 203211-100G
Erbium(III) chloride	$ErCl_3{\cdot}6H_2O$	99.9% trace metals basis	crystals and lumps	289256-25G 289256-100G
Erbium(III) fluoride	ErF_3	99.99% trace metals basis	powder	432156-5G
Erbium(III) iodide	ErI_3	99.9% trace metals basis	powder	439789-1G 439789-5G
Europium(III) bromide	$EuBr_3 \cdot xH_2O$	≥99.99% trace metals basis	solid	575259-5G
Europium(II) chloride	$EuCl_2$	99.99% trace metals basis	powder and chunks	431850-1G 431850-5G
Europium(III) chloride	$EuCl_3$	99.99% trace metals basis	powder	429732-1G 429732-5G
Europium(III) chloride	$EuCl_3$	≥99.9% trace metals basis	powder	238066-1G 238066-10G
Europium(III) chloride	$EuCl_3 \cdot 6H_2O$	99.99% trace metals basis	crystals and lumps	203254-1G 203254-5G 203254-25G
Europium(III) chloride	$EuCl_3 \cdot 6H_2O$	99.9% trace metals basis	crystals and lumps	212881-5G 212881-25G
Europium(III) fluoride	EuF_3	99.99% trace metals basis	powder	449806-1G 449806-5G
Europium(II) iodide	EuI_2	99.9% trace metals basis	powder	474770-1G 474770-5G
Gadolinium(III) bromide	$GdBr_3$	99.99% trace metals basis	powder	485020-2G
Gadolinium(III) bromide	$GdBr_3 \cdot xH_2O$	99.99% trace metals basis	powder and chunks	451118-10G 451118-50G
Gadolinium(III) chloride	$GdCl_3$	99.99% trace metals basis	powder	439770-5G 439770-25G
Gadolinium(III) chloride	$GdCl_3 \cdot 6H_2O$	99.999% trace metals basis	crystals and lumps	203289-1G 203289-5G 203289-25G
Gadolinium(III) chloride	$GdCl_3 \cdot 6H_2O$	99%, titration	powder	G7532-5G G7532-25G

Name	Formula	Purity	Physical Form	Prod. No.
Gadolinium(III) chloride	$GdCl_3 \cdot xH_2O$	99.99% trace metals basis	solid	450855-10G 450855-50G
Gadolinium(III) fluoride	GdF_3	99.99% trace metals basis	powder	432164-5G 432164-25G
Gadolinium(III) iodide	GdI_3	99.99% trace metals basis	powder	466298-1G
Holmium(III) bromide	$HoBr_3$	99.99% trace metals basis	powder	439762-5G
Holmium(III) bromide	$HoBr_3 \cdot xH_2O$	99.999% trace metals basis	powder and chunks	575232-5G 575232-25G
Holmium(III) chloride	$HoCl_3$	99.9% trace metals basis	powder	450901-1G 450901-5G
Holmium(III) chloride	$HoCl_3 \cdot 6H_2O$	99.9% trace metals basis	crystals and lumps	289213-5G 289213-25G
Holmium(III) fluoride	HoF_3	99.99% trace metals basis	powder	432075-10G
Lanthanum(III) bromide	$LaBr_3 \cdot xH_2O$	≥99.99% trace metals basis	powder and chunks	575275-5G 575275-25G
Lanthanum(III) chloride	$LaCl_3 \cdot 7H_2O$	99.999% trace metals basis	solid	203521-25G 203521-100G
Lanthanum(III) chloride	$LaCl_3 \cdot xH_2O$	99.9% trace metals basis	powder and chunks	211605-100G 211605-500G
Lanthanum(III) fluoride	LaF_3	99.99% trace metals basis	powder	449857-5G 449857-25G 449857-100G
Lanthanum(III) iodide	LaI_3	99.9%	powder	466093-1G
Lutetium(III) bromide	$LuBr_3$	99.99%	powder	587133-1G
Lutetium(III) bromide	$LuBr_3 \cdot xH_2O$	99.999%	-	545066-1G
Lutetium(III) chloride	$LuCl_3$	99.99% trace metals basis	powder	450960-1G 450960-5G
Lutetium(III) chloride	$LuCl_3 \cdot 6H_2O$	≥99.99% trace metals basis	crystalline	542075-1G 542075-5G
Lutetium(III) chloride	$LuCl_3 \cdot 6H_2O$	99.9% trace metals basis	crystalline	298131-1G
Lutetium(III) fluoride	LuF_3	99.99% trace metals basis	powder	432113-1G 432113-5G
Lutetium(III) iodide	LuI_3	99.9% trace metals basis	powder	460575-5G
Neodymium(III) bromide	$NdBr_3$	99.9% trace metals basis	powder	439711-5G 439711-25G
Neodymium(III) chloride	$NdCl_3$	≥99.99% trace metals basis	powder	449946-5G 449946-25G
Neodymium(III) chloride	$NdCl_3 \cdot 6H_2O$	99.9% trace metals basis	crystals and lumps	289183-25G
Neodymium(III) fluoride	NdF_3	99.99% trace metals basis	powder	449954-10G
Neodymium(II) iodide	NdI_2	≥99.9% trace metals basis	powder	652431-1G 652431-5G
Neodymium(III) iodide	NdI_3	99.9%	powder	659215-1G 659215-5G
Praseodymium(III) bromide	$PrBr_3$	99.99% trace metals basis	powder	439703-2G 439703-10G
Praseodymium(III) bromide	$PrBr_3 \cdot xH_2O$	≥99.99% trace metals basis	chunks	575267-5G
Praseodymium(III) chloride	$PrCl_3$	99.99% trace metals basis	powder	298298-5G 298298-25G
Praseodymium(III) chloride	$PrCl_3 \cdot xH_2O$	99.9% trace metals basis	solid	205141-10G 205141-50G
Praseodymium(III) fluoride	PrF_3	99.99% trace metals basis	powder	432091-5G
Samarium(III) bromide	$SmBr_3$	99.9% trace metals basis	powder	416630-5G 416630-25G
Samarium(III) chloride	$SmCl_3$	99.9%	powder	400610-2G 400610-10G
Samarium(III) chloride	$SmCl_3 \cdot 6H_2O$	≥99.99% trace metals basis	crystalline	204277-5G
Samarium(III) chloride	$SmCl_3 \cdot 6H_2O$	≥99%	powder and chunks	248800-10G 248800-50G
Samarium(II) iodide	SmI_2	≥99.9% trace metals basis	powder	409340-1G 409340-5G
Samarium(II) iodide	SmI_2	-	liquid	347116-25ML 347116-100ML 347116-800ML 347116-4X10ML
Samarium(III) iodide	SmI_3	-	powder	484032-1G
Scandium(III) bromide	$ScBr_3$	≥99.99% trace metals basis	powder	517526-1G
Scandium(III) chloride	$ScCl_3$	99.99% trace metals basis	powder	451266-1G 451266-5G

Name	Formula	Purity	Physical Form	Prod. No.
Scandium(III) chloride	$ScCl_3$	99.9% trace metals basis	powder	409359-1G 409359-5G
Scandium(III) chloride	$ScCl_3 \cdot 6H_2O$	99.999% trace metals basis	powder	451274-1G
Scandium(III) fluoride	ScF_3	99.99% trace metals basis	powder	432105-1G 432105-5G
Scandium(III) iodide	ScI_3	99.999% trace metals basis	powder	439673-1G
Terbium(III) bromide	$TbBr_3$	99.99% trace metals basis	powder	466344-1G
Terbium(III) chloride	$TbCl_3$	99.99% trace metals basis	powder	451304-1G 451304-10G
Terbium(III) chloride	$TbCl_3$	99.9% trace metals basis	powder	439657-2G 439657-10G
Terbium(III) chloride	$TbCl_3 \cdot 6H_2O$	99.999% trace metals basis	powder and chunks	204560-1G 204560-5G
Terbium(III) chloride	$TbCl_3 \cdot 6H_2O$	99.9% trace metals basis	solid	212903-5G 212903-25G
Terbium(III) chloride	$TbCl_3 \cdot xH_2O$	99.99% trace metals basis	solid	451312-5G
Terbium(III) fluoride	TbF_3	99.99% trace metals basis	powder	432067-1G 432067-5G
Terbium(III) iodide	TbI_3	99.99% trace metals basis	flakes	427098-1G 427098-5G
Thulium(III) bromide	$TmBr_3$	99.99%	powder	439630-1G
Thulium(III) chloride	$TmCl_3$	99.9% trace metals basis	powder	439649-1G 439649-5G
Thulium(III) chloride	$TmCl_3 \cdot 6H_2O$	99.99% trace metals basis	powder	204668-1G 204668-5G
Thulium(III) fluoride	TmF_3	99.99%	powder	432148-1G 432148-5G
Ytterbium(III) bromide	$YbBr_3$	99.99% trace metals basis	powder	451320-1G 451320-5G
Ytterbium(III) bromide	$YbBr_3 \cdot xH_2O$	-	pellets	544965-5G
Ytterbium(III) chloride	$YbCl_3$	99.99% trace metals basis	beads	450073-5G 450073-25G
Ytterbium(III) chloride	$YbCl_3$	99.9%	powder	439614-5G 439614-25G
Ytterbium(III) chloride	$YbCl_3 \cdot 6H_2O$	99.998% trace metals basis	powder and chunks	204870-10G 204870-50G
Ytterbium(III) chloride	$YbCl_3 \cdot 6H_2O$	99.9% trace metals basis	crystals and lumps	337927-10G 337927-50G
Ytterbium(III) fluoride	YbF_3	99.98% trace metals basis	powder	432121-10G 432121-50G
Ytterbium(II) iodide	YbI_2	≥99.9% trace metals basis	powder	494372-1G 494372-5G
Yttrium(III) chloride	YCl_3	99.99% trace metals basis	powder	451363-10G 451363-50G
Yttrium(III) chloride	$YCl_3 \cdot 6H_2O$	99.999% trace metals basis	solid	204919-10G 204919-50G
Yttrium(III) chloride	$YCl_3 \cdot 6H_2O$	99.99% trace metals basis	powder	464317-25G 464317-100G
Yttrium(III) chloride	$YCl_3 \cdot 6H_2O$	99.9% trace metals basis	crystals and lumps	211648-50G 211648-250G
Yttrium(III) fluoride	YF_3	99.99% trace metals basis	powder	451371-10G
Yttrium(III) iodide	YI_3	99.9% trace metals basis	flakes	413011-1G

Rare Earth Nitrates

Name	Formula	Purity	Physical Form	Prod. No.
Ammonium cerium(IV) nitrate	$Ce(NH_4)_2(NO_3)_6$	≥99.99% trace metals basis	crystalline	229547-10G 229547-50G 229547-250G
Cerium(III) nitrate	$Ce(NO_3)_3 \cdot 6H_2O$	99.999% trace metals basis	crystals and lumps	202991-25G 202991-125G
Cerium(III) nitrate	$Ce(NO_3)_3 \cdot 6H_2O$	99.99% trace metals basis	crystals and lumps	392219-25G 392219-100G
Cerium(III) nitrate	$Ce(NO_3)_3 \cdot 6H_2O$	99% trace metals basis	crystals and lumps	238538-100G 238538-500G
Dysprosium(III) nitrate	$Dy(NO_3)_3 \cdot xH_2O$	99.9% trace metals basis	crystals and lumps	298158-25G 298158-100G
Erbium(III) nitrate	$Er(NO_3)_3 \cdot 5H_2O$	99.9% trace metals basis	crystals and lumps	298166-25G 298166-100G
Europium(III) nitrate	$Eu(NO_3)_3 \cdot 5H_2O$	99.9% trace metals basis	crystals and lumps	207918-1G 207918-10G 207918-50G
Europium(III) nitrate	$Eu(NO_3)_3 \cdot xH_2O$	99.99% trace metals basis	solid	254061-1G 254061-10G

Name	Formula	Purity	Physical Form	Prod. No.
Gadolinium(III) nitrate	$Gd(NO_3)_3 \cdot 6H_2O$	99.99% trace metals basis	solid	451134-10G 451134-50G
Gadolinium(III) nitrate	$Gd(NO_3)_3 \cdot 6H_2O$	99.9% trace metals basis	crystals and lumps	211591-25G 211591-100G
Holmium(III) nitrate	$Ho(NO_3)_3 \cdot 5H_2O$	99.9% trace metals basis	solid	325732-10G 325732-50G
Lanthanum(III) nitrate	$La(NO_3)_3 \cdot 6H_2O$	≥99.0%, titration	crystalline	61520-100G-F 61520-500G-F
Lanthanum(III) nitrate	$La(NO_3)_3 \cdot 6H_2O$	99.999% trace metals basis	solid	203548-25G 203548-100G 203548-500G
Lanthanum(III) nitrate	$La(NO_3)_3 \cdot 6H_2O$	99.99% trace metals basis	solid	331937-5G 331937-100G 331937-500G
Lanthanum(III) nitrate	$La(NO_3)_3 \cdot xH_2O$	99.9% trace metals basis	powder and chunks	238554-100G 238554-500G
Lutetium(III) nitrate	$Lu(NO_3)_3 \cdot xH_2O$	99.999% trace metals basis	solid	542067-5G
Lutetium(III) nitrate	$Lu(NO_3)_3 \cdot xH_2O$	99.9% trace metals basis	crystals and lumps	436429-1G 436429-5G
Neodymium(III) nitrate	$Nd(NO_3)_3 \cdot 6H_2O$	99.9% trace metals basis	crystalline	289175-25G 289175-100G
Praseodymium(III) nitrate	$Pr(NO_3)_3 \cdot 6H_2O$	99.9% trace metals basis	crystalline	205133-10G 205133-50G 205133-250G
Samarium(III) nitrate	$Sm(NO_3)_3 \cdot 6H_2O$	99.9% trace metals basis	powder and chunks	298123-25G 298123-100G
Terbium(III) nitrate	$Tb(NO_3)_3 \cdot 5H_2O$	99.9% trace metals basis	solid	325945-5G 325945-25G
Terbium(III) nitrate	$Tb(NO_3)_3 \cdot 6H_2O$	99.999% trace metals basis	crystals and lumps	217212-2G 217212-10G
Ytterbium(III) nitrate	$Yb(NO_3)_3 \cdot 5H_2O$	99.999%	chunks	217220-5G 217220-25G
Ytterbium(III) nitrate	$Yb(NO_3)_3 \cdot 5H_2O$	99.9% trace metals basis	crystals and lumps	209147-10G 209147-50G

Rare Earth Acetates and Acetylacetonates

Name	Formula	Purity	Physical Form	Prod. No.
Cerium(III) acetate	$Ce(CH_3CO_2)_3 \cdot xH_2O$	99.9% trace metals basis	powder and chunks	367753-50G 367753-250G
Cerium(III) acetylacetonate	$Ce(C_5H_7O_2)_3 \cdot xH_2O$	-	crystalline powder	381403-50G 381403-250G
Europium(III) acetate	$Eu(CH_3CO_2)_3 \cdot xH_2O$	99.9% trace metals basis	powder	325627-5G 325627-25G
Gadolinium(III) acetate	$Gd(CH_3CO_2)_3 \cdot xH_2O$	99.9% trace metals basis	crystalline powder	325678-25G 325678-100G
Gadolinium(III) acetylacetonate	$Gd(C_5H_7O_2)_3 \cdot xH_2O$	99.9% trace metals basis	powder	331716-5G 331716-25G
Lanthanum(III) acetate	$La(CH_3CO_2)_3 \cdot xH_2O$	99.9% trace metals basis	crystalline powder	306339-100G 306339-500G
Lanthanum(III) acetylacetonate	$La(C_5H_7O_2)_3 \cdot xH_2O$	-	powder	325759-10G 325759-100G
Terbium(III) acetate	$Tb(CH_3CO_2)_3 \cdot xH_2O$	99.9% trace metals basis	crystals and lumps	325929-5G 325929-25G
Ytterbium(III) acetate	$Yb(C_2H_3O_2)_3 \cdot 4H_2O$	99.9% trace metals basis	powder and chunks	326011-10G 326011-50G

High-Purity Beaded Rare Earth Materials

Aldrich®-produced beaded materials offer the advantage of high purity (trace metals basis) as well as ease of handling and delivery. Rare earth metal salts find applications in a variety of areas including:

- Alternative energy
- Electronics
- Biomedical applications
- Sensors
- Scintillation devices

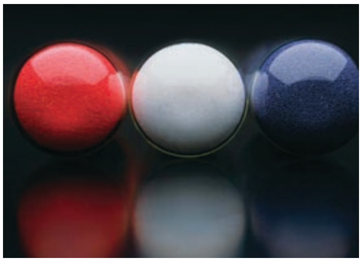

Name	Formula	Purity (Trace Metals Basis)	Prod. No.
Cerium(III) chloride, anhydrous	$CeCl_3$	99.9%	298190
Cerium(III) chloride, anhydrous	$CeCl_3$	≥99.9%	450731
Cerium(III) chloride, anhydrous	$CeCl_3$	≥99.99%	429406
Cerium(III) bromide, anhydrous	$CeBr_3$	99.99%	563226
Cerium(III) iodide, anhydrous	CeI_3	99.99%	466085
Lanthanum(III) chloride, anhydrous	$LaCl_3$	99.9%	298182
Lanthanum(III) chloride, anhydrous	$LaCl_3$	≥99.99%	449830
Lanthanum(III) bromide, anhydrous	$LaBr_3$	≥99.99%	449822
Lanthanum(III) iodide, anhydrous	LaI_3	99.9%	413674
Praseodymium(III) chloride, anhydrous	$PrCl_3$	99.99%	451215
Neodymium(III) bromide, anhydrous	$NdBr_3$	99.99%	466115
Samarium(III) chloride, anhydrous	$SmCl_3$	99.99%	449997
Samarium(III) bromide, anhydrous	$SmBr_3$	99.99%	451231
Ytterbium(III) chloride, anhydrous	$YbCl_3$	99.99%	450073
Yttrium(III) chloride, anhydrous	YCl_3	99.99%	450103

For detailed product information and inquiries about custom-designed materials, contact us at matsci@sial.com

Discovery and Single Crystal Growth of Lanthanide Intermetallics—Interplay of Synthesis and Physical Properties



Devin C. Schmitt, Michael J. Kangas, Julia Y. Chan*
Louisiana State University, Department of Chemistry
232 Choppin Hall, Baton Rouge, LA 70803
*Email: jchan@lsu.edu

Correlated Systems

Solid state and materials chemistry have made a tremendous impact and have experienced growth in recent years, particularly for rare earth-containing materials. This is motivated by the potential applications impacting a vast number of areas in materials research. Materials containing *f*-orbital electrons are ubiquitous in technological applications involving electronic, magnetic, thermal, and optical properties. We have been able to exploit the self-flux growth techniques[1,2] to grow single crystals over the last several years. Synthesis of solid-state materials by flux growth has made a significant impact in both fundamental and application-driven research and is part of the National Academy of Science grand challenge,[3] specifically highly correlated materials, a class of materials with strong electron-electron interactions. A *Physics Today* article highlighted the need for high quality single crystals necessary for the discovery of novel materials with interesting properties.[4] A good read is also "Fishing the Fermi Sea", which describes the importance of making highly correlated materials in single crystal form.[5]

To understand the chemistry and physics of compounds with *f*-electrons, it is vital that materials be made in single crystal form so intrinsic properties can be studied. This involves methods such as self-flux growth, Czochralski, hydrothermal, and microwave methods. Our work has been motivated by the various functional classes of materials. In this review, we will highlight several classes of materials, including highly correlated and energy materials containing lanthanide elements—specifically synthesized by flux growth.

The focus of our research over the last several years has primarily been crystal growth of highly correlated intermetallics with Group 13-15 main group elements (**Figure 1**).[6] We have discovered and worked on compounds that show heavy electron mass behavior (containing Ce) and compounds that exhibit unusual magnetism. While most materials are serendipitously discovered, systematic and rational methods must be developed.[6]

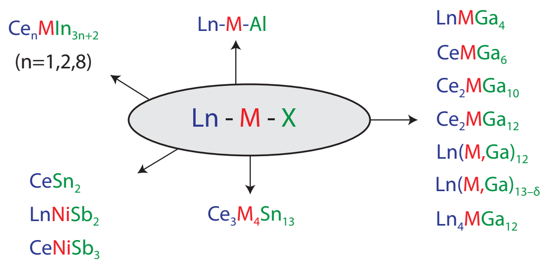

Figure 1. Representative lanthanide intermetallic materials illustrating the range of stoichiometries obtainable through molten metal flux growth. Lanthanide metals, transition metals, and flux elements are denoted in blue, red, and green, respectively.

Highly correlated systems have generated much interest, especially in the search for quantum materials, unconventional superconductors, and magnetic materials. Many of the compounds and systems discovered in this group are also highly field dependent, exhibiting large magnetoresistance, and showing unusual anisotropic magnetic behavior. While Ce-containing intermetallics have attracted much attention in the past, these unusual phenomena have also been extended to Pr- and Yb-based intermetallic phases. The skutterudites PrM_4Pn_{12} (M = Fe, Ru, or Os; Pn = P, As, Sb), $Pr(Cu,Ga)_{13}$, and $PrAgIn_2$ have been studied because of diverse behavior such as superconductivity, unusual magnetic ground states and heavy electron behavior. Only with high quality single crystals can the origin of these properties be elucidated.

More recently, magnetization measurements of the ultrapure *f*-electron-based superconductor β-$YbAlB_4$[7] demonstrate zero field quantum criticality without tuning external parameters such as high magnetic fields and pressures in a metal.[8] These properties can only be determined with clean and high-quality materials.

Energy Applications

Lanthanide-containing compounds are not only interesting for fundamental science but can have direct implications in device-level applications. On the energy front, fields such as refrigeration and power generation have traditionally been dominated by mechanical phase-change technologies with relatively low efficiencies. A general drive in the materials and engineering community has been to replace these devices by thermoelectric and magnetocaloric solid-state materials with equal or higher efficiencies and much lower failure rates. Due to interesting magnetic properties and high atomic weight, lanthanide-containing compounds, or rare earths, are excellent candidates for thermoelectric and magnetocaloric materials, respectively.

Thermoelectric Materials

Thermoelectrics are materials with the ability to convert thermal energy to electrical energy or use electrical energy to produce a temperature gradient. Their efficiency is measured by the dimensionless figure of merit *ZT*, which has components of electrical conductivity, Seebeck coefficient, and thermal conductivity. Characteristics of an ideal thermoelectric material include low thermal conductivity similar to a glass and high thermoelectric power factor (the product of electrical conductivity and Seebeck coefficient squared). To date, the best thermoelectric materials have *ZT* between 1 and 2, but a *ZT* ~4 is needed for competitive cooling and power generation.

$YbAl_3$ is an example of the potential for rare earth-based intermetallic compounds for thermoelectric materials. $YbAl_3$ has a thermoelectric power factor of 180 $\mu W/K^2$-cm at 300 K due to Yb valence fluctuations; the highest known value for any thermoelectric material. However, due to very high thermal conductivity at room temperature, $YbAl_3$ is not a suitable thermoelectric material.[9] We can visualize this by considering thermal conductivity as a parasitic value. The higher the thermal conductivity, the more heat is allowed to leach through the system without contributing to voltage generation. In cooling applications, high thermal conductivity translates into a relatively small temperature

gradient that can be established between the hot and cold sides of the device. If, however, we were able to keep the power factor of $YbAl_3$ constant and reduce the thermal conductivity to as low as a glass (~1 W/m-K), we would find a ZT of 5.4 at room temperature—competitive with residential-grade refrigeration devices but with greatly increased longevity. Alternatively, as a power generating device, a ZT of 5.4 would correspond to >40% higher fuel efficiency in an automobile (using similar estimates to that of Bell).[10]

Rare earth-containing thermoelectrics not only have the benefit of potential valence instabilities, but they can form complex structures and have high atomic masses, both of which contribute to a significant reduction in thermal conductivity, which can improve performance as a thermoelectric. Substitution of the isovalent, but much higher atomic mass Yb for Ca in $Ca_{14}MnSb_{11}$ led to $Yb_{14}MnSb_{11}$.[11] $Yb_{14}MnSb_{11}$ is a complex Zintl intermetallic material with a high thermoelectric power factor at elevated temperatures and a low room temperature lattice thermal conductivity of ~0.45 W/m-K, partly due to the high average atomic mass of the material. Optimized $Yb_{14}MnSb_{11}$ is the highest performing elevated temperature p-type thermoelectric material to date, with a ZT >1 at 1,200 K.[12]

Rare earths can be used to tune the electronic structure of a material. The Co_4Sb_{12} skutterudite (**Figure 2**) is a small bandgap semiconductor with a large thermoelectric power factor. The thermal conductivity of Co_4Sb_{12} is far too high for thermoelectric applications (>10 W/m-K), but the skutterudite structure contains voids large enough for rare earth atoms to reside. Rare earth ions act as both charge donors to modify electronic properties and phonon scattering centers to significantly reduce thermal conductivity. Iron can then be substituted for Co to return the compound to a semiconducting state. The filled skutterudite $Ce(Co,Fe)_4Sb_{12}$ has a large thermoelectric power factor, partly due to *f*- and *d*-electron hybridization, and a greatly reduced thermal conductivity, leading to ZT ~1 at room temperature.[13]

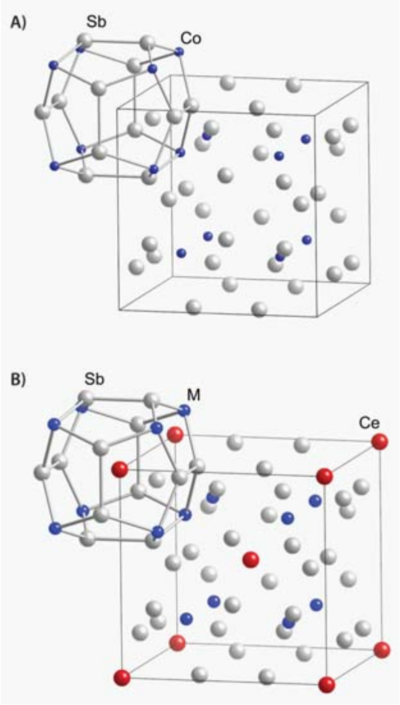

Figure 2. Crystal structures of the unfilled (A) and filled (B) skutterudite structure illustrating the filling of voids by lanthanide elements (example: Co_4Sb_{12} and $Ce(Co,Fe)_4Sb_{12}$). Blue spheres represent the transition metal (Co or Fe). Grey and red spheres represent Sb and Ce, respectively

The goal of a ZT >4 in order to provide competitive materials for cooling/power generation in bulk materials is not unrealistic, as Goldsmid proposes.[14] This "limiting" factor was set using the best values of the parameters in ZT (ρ, S, and κ) found for bulk materials. Indeed, these values are conservative, and the estimation will likely increase as new thermoelectric materials are discovered. The high atomic masses and potential valence instabilities of rare earth containing intermetallic compounds make them ideal candidates for reaching the goal of ZT >4.

Magnetocaloric Materials

The magnetocaloric effect offers the possibility of an efficient and environmentally friendly refrigeration technology, and is based on utilizing the entropy changes (ΔS_m) due to magnetic spins aligning in an applied field. This effect is caused by the coupling of the magnetic sublattice with the magnetic field, leading to the change in the magnetic part of the entropy of a solid. Cooling based on the magnetocaloric effect has already been demonstrated, but research is needed to find magnetocaloric materials with improved properties. An ideal magnetocaloric material should possess (1) a large magnetic moment so the entropy change will be large when the spins order and (2) a magnetic ordering temperature in the relevant temperature range. Other properties include high thermal conductivity, good mechanical properties, low cost and low toxicity. Rare earth compounds are excellent candidates because they not only possess large magnetic moments but can be easily optimized via substitution with other rare earth elements. Gd metal and its alloys show a large magnetocaloric effect near room temperature and are frequently used as benchmark.

A great number of binary, ternary, and quaternary rare earth-containing intermetallics have been investigated and reviewed recently.[15,16] The materials range from being active at a few tens of Kelvin to above room temperature and exhibit many types of magnetic transitions. Magnetocaloric properties in Gd_5Si_4 and $Gd_5(Si_xGe_{1-x})_4$ alloy (Aldrich Prod. Nos. 693510, 693502) based materials have been reviewed.[17] These compounds order ferromagnetically near room temperature. In these materials, the magnetic entropy change is enhanced due to the combination of the magnetic ordering at the desired temperature coinciding with a structure change.

$La(Fe_{1-x}Si_x)_{13}$ alloys have been shown to be effective magnetocaloric materials near room temperature. The magnetic properties can be tuned by doping both the *Ln* and Fe/Si sites, as well as through the incorporation of light elements into interstitial sites. In these compounds, the ordering temperature increases linearly with lattice expansion. Interestingly, in this structure type, the magnetic transition can be first order or second order depending on composition.[18]

Anisotropic properties are also important in magnetocaloric materials. In the oxide $ErAlO_3$, orienting the crystal along the **c** axis more than doubles the magnetic entropy change compared to the **a** or **b** axes, with ΔS_m of approximately -180, -70 and -80 mJ/cm^3-K for a 2T change.[19] In addition to optimizing the magnetocaloric effect by orienting single crystals along select crystal axes, changing the orientation of single crystals in a fixed magnetic field can exhibit the magnetocaloric effect. This effect is termed the anisotropic magnetocaloric effect. In $DyNi_2$, the effect is slightly larger for a change from [001] - [110] in a constant field of 2 T than for a polycrystalline sample in a field change of 0-2 T, with ΔS_m values of approximately -132 and -110 mJ/ cm^3-K, respectively.[20]

Synthesis

The majority of samples characterized for magnetocaloric and thermoelectric applications are polycrystalline and have been synthesized through arc-melting or other high temperature methods. Arc-melting allows precision doping and tuning of magnetic and electronic properties by stoichiometric weighing of reactants. Polycrystalline samples contain many crystallites oriented in all directions, providing an average of the magnetocaloric effect and an overall reduction in thermal conductivity for thermoelectric applications due to boundary scattering. However, the growth of single crystals through flux growth or other techniques presents a number of advantages that include more complete structural characterization and determination of anisotropic magnetic and electrical properties. Single crystals can be oriented to the direction that maximizes the magnetic entropy change or the carrier mobility in anisotropic materials.

For example, we have grown high quality single crystals of $CePdGa_6$, Ce_2PdGa_{10}, and Ce_2PdGa_{12} using the self-flux method by reacting high purity Ce (Aldrich Prod. No. 263001) and Pd (Aldrich Prod. No. 203939) in excess Ga (Aldrich Prod. No. 203319) as a reactive flux in a 1:1:20 ratio. Elements are placed in an alumina crucible, sealed in an evacuated fused silica tube, then heated to a maximum dwell temperature of 1,423 K. They are then slowly cooled to the desired spin temperature, centrifuged, and subsequently etched to remove residual Ga flux. The reaction products, in this case, depend solely on the spin temperature selected (**Figure 3**). Larger crystals of $CePdGa_6$ were grown using an alternate temperature profile and a reaction ratio of 2:3:30.[6]

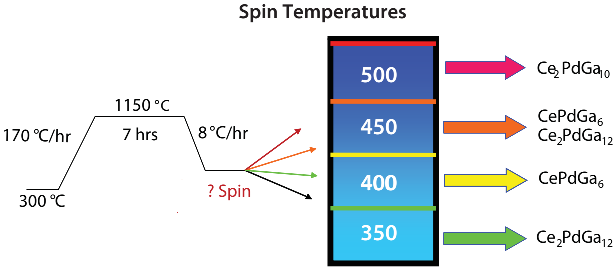

Figure 3. Heating profiles for the synthesis of single crystalline Ce-Pd-Ga phases. Different spin temperatures yielded different stoichiometries, as indicated by varying spin/quench temperatures.

High quality single crystals of each ternary phase were characterized by single-crystal X-ray diffraction. As shown in **Figure 4**, each compound adopts a distinct tetragonal structure. $CePdGa_6$, a heavy-fermion material, crystallizes in space group *P4/mmm* with $a = b = 4.350(3)$ Å and $c = 7.9230(5)$ Å. Ce_2PdGa_{10} adopts a different tetragonal structure (*I4/mmm*) with lattice constants $a = b = 4.3230(3)$ Å and $c = 26.536(3)$ Å. Finally, Ce_2PdGa_{12}, an antiferromagnetic material, crystallizes in space group *P4/nbm* with lattice parameters $a = b = 6.1040(2)$ Å and $c = 15.5490(6)$ Å.

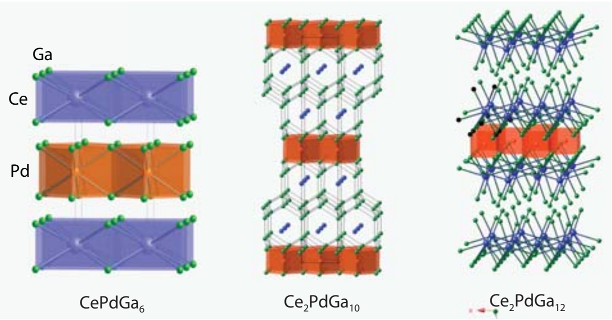

Figure 4. Crystal structures for $CePdGa_6$, Ce_2PdGa_{10}, and Ce_2PdGa_{12}. Blue, orange, and green spheres represent Ce, Pd, and Ga atoms, respectively.

Starting stoichiometry also plays a key role in determining the structure of the final product, as seen in the case of Cu-containing lanthanide intermetallics. By changing the initial reaction ratio from 1:1:20 to 1:5:20, three different structure types are stabilized (**Figure 5**), yielding phases that exhibit properties ranging from heavy-fermion behavior to large positive magnetoresistance. By controlling both the reaction/spin temperatures as well as the starting stoichiometries, a wide range of possible structures are accessible through the metal flux technique.

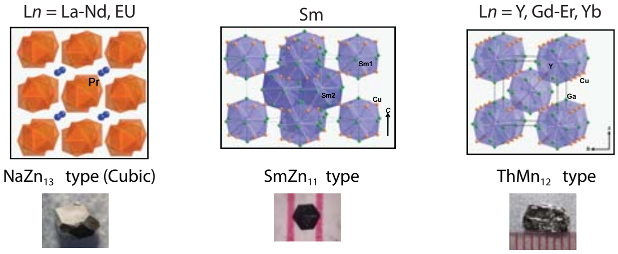

Figure 5. Changing the reaction ratio of *Ln*:Cu:flux to 1:5:20, three additional structure types are stabilized: $NaZn_{13}$ type, $SmZn_{11}$ type, and $ThMn_{12}$ type (left to right).

Conclusions

The search is just beginning—the lanthanides are a truly functional toolbox for the discovery of novel materials with properties that are just yet to be discovered and understood.

Acknowledgments

The authors acknowledge NSF-DMR0237664, NSF-DMR0756281, and NSF-DMR1063735 for funding and the Chan Research Group for useful discussion.

References

(1) Canfield, P.C.; Fisk, Z. *Philos. Mag. B-Phys. Condens. Matter Stat. Mech. Electron. Opt. Magn. Prop.* 1992, *65*, 1117.
(2) Kanatzidis, M.G.; Pöttgen, R.; Jeitschko, W. *Angew. Chem. Int. Ed. Engl.* **2005**, *44*, 6996.
(3) *Frontiers in Crystalline Matter: from Discovery to Technology*; The National Academies Press: Washington, D.C., 2009.
(4) Feder, T. *Physics Today* **2007**, 60(8), 26.
(5) Canfield, P.C., *Nat. Phys.* **2008**, *4*, 167.
(6) Thomas, E.L.; Millican, J.N.; Okudzeto, E.K.; Chan, J.Y. *Comments Inorg. Chem.* **2006**, *27*, 1.
(7) Macaluso, R.T.; Nakatsuji, S.; Kuga, K.; Thomas, E.L.; Machida, Y.; Maeno, Y.; Fisk, Z.; Chan, J.Y. *Chem. Mater.* **2007**, *19*, 1918.
(8) Matsumoto, Y.; Nakatsuji, S.; Kuga, K.; Karaki, Y.; Horie, N.; Shimura, Y.; Sakakibara, T.; Nevidomskyy, A.H.; Coleman, P. *Science* **2011**, *331*, 316.
(9) Mahan, G. D., Good thermoelectrics. In *Solid State Physics, Vol 51*, Academic Press Inc: San Diego, 1998; Vol. 51, pp 81-157.
(10) Bell, L. E. *Science* **2008**, *321*, 1457.
(11) Chan, J.Y.; Olmstead, M.M.; Kauzlarich, S.M.; Webb, D.J. *Chem. Mater.* **1998**, *10*, 3583.
(12) Kauzlarich, S.M.; Brown, S.R.; Snyder, G.J. *Dalton Trans.* **2007**, 2099.
(13) Nolas, G.S.; Morelli, D.T.; Tritt, T.M. *Annu. Rev. Mater. Sci.* **1999**, *29*, 89.
(14) Goldsmid, H.J. A new upper limit to the figure of merit. In *Thermoelectrics Handbook: Macro to Nano*, Rowe, D.M., Ed.; CRC Press: Boca Raton, 2006; pp 1-14.
(15) Gschneidner, K.A., Jr. et al. *Rep. Prog. Phys.* **2005**, *68*, 1479.
(16) Gschneidner, K.A., Jr.; Pecharsky, V.K. *Annu. Rev. Mater. Sci.* **2000**, *30*, 387.
(17) Pecharsky, V.K.; Gschneidner, K.A., Jr. *J. Mag. Magn. Mater.* **1999**, *200*, 44.
(18) Shen, B.G.; Sun, J.R.; Hu, F.X.; Zhang, H.W.; Cheng, Z.H., *Adv. Mater.* **2009**, *21*, 4545.
(19) Kimura, H.; Numazawa, T.; Sato, M.; Ikeya, T.; Fukuda, T.; Fujioka, K. *J. Mater. Sci.* **1997**, *32*, 5743.
(20) Plaza, E.J.R.; de Sousa, V.S.R.; Reis, M.S.; von Ranke, P.J. *J. Alloy. Compd.* **2010**, *505*, 357.

High-Purity Metals for Molten Flux Growth

For a complete list of available materials, visit Aldrich.com/periodic

Name	**M.P. (°C)**	**Purity (Trace Metals Basis)**	**Form, Approx. Piece Size**	**Prod. No.**
Gallium	29.8	99.9995%	(metallic liquid or solid (ambient temp dependent))	203319-1G 203319-5G 203319-25G
Gallium	29.8	99.999%	(metallic liquid or solid (ambient temp dependent))	263273-10G 263273-50G
Gallium	29.8	99.99%	(metallic liquid or solid (ambient temp dependent))	263265-10G 263265-50G
Indium	155-158	99.999%	beads	264113-5G 264113-25G
Indium	155-158	99.999%	powder, −60 mesh	203432-5G 203432-25G
Indium	155-158	99.99%	pieces, ¼ - 2 in.	326615-50G
Indium	155-158	99.99%	powder, −100 mesh	264032-5G 264032-25G
Tin	231.9	99.999%	shot	204692-10G
Lead	327.4	99.995%	shot, 1 - 3 mm	695912-25G
Lead	327.4	99.95%	powder, −100 mesh	391352-100G
Aluminum	660.37	≥99.999%	pellets, 3 - 8 mesh	326941-25G
Aluminum	660.37	99.99%	pellets, 3 - 8 mesh	338788-50G
Aluminum	660.37	≥99.95%	powder, <75 μm	202584-10G
Aluminum	660.37	99.99%	flakes, 1 mm	518573-500G

Intermetallics and Alloys for Magnetic Refrigeration

For more information, visit Aldrich.com/magnetocaloric

Name	**Chemical Composition**	**Physical Form**	**Curie Temperature**	**Prod. No.**
Dysprosium-Erbium-Aluminum alloy	$Dy_{0.8}Er_{0.2}Al_2$	powder	below 60 K	693499-1G
Gadolinium	-	ingot	293 K	691771-10G
Gadolinium-silicon-germanium alloy	$Gd_5Si_2Ge_2$	powder and chunks	~270 K	693510-1G
Gadolinium-silicon-germanium alloy	$Gd_5Si_{0.5}Ge_{3.5}$	powder and chunks	~70 K	693502-1G

Rare Earth-based Permanent Magnets

For more information, visit Aldrich.com/magnetic

Name	**Composition**	**Form**	**Properties**	**Prod. No.**
Samarium-cobalt alloy 18	Cobalt 62.75 wt. % Samarium 37.25 wt. %	disc, 10 × 6 mm	Magnetic parameters/properties: Maximum Energy Product (BH): 140 kJ/m^3 (18 MGsOe) Residual Induction (Br): 0.87 T (8.7 kGs) Coercive Force (Hc): 680 kA/m (8.5 kOe) Intrinsic Coercive Force (Hci): 2390 kA/m (30.0 kOe)	692859-3EA
Samarium-cobalt alloy 24	Cobalt 49.05 wt. % Iron 17.25 wt. % Samarium 25 wt. % Zirconium 2.75 wt. % copper 5.95 wt. %	disc, 10 × 6 mm	Magnetic parameters/properties: Maximum Energy Product (BH): 190 kJ/m^3 (24 MGsOe) Residual Induction (Br): 1.00 T (10.0 kGs) Coercive Force (Hc): 740 kA/m (9.3 kOe) Intrinsic Coercive Force (Hci): 2070 kA/m (26.0 kOe)	692840-3EA
Samarium-cobalt alloy 30	Cobalt 48.1 wt. % Iron 19.25 wt. % Samarium 25 wt. % Zirconium 2.75 wt. % copper 4.9 wt. %	disc, 10 × 6 mm	Magnetic parameters/properties: Maximum Energy Product (BH): 240 kJ/m^3 (30 MGsOe) Residual Induction (Br): 1.13 T (11.6 kGs) Coercive Force (Hc): 840 kA/m (10.6 kOe) Intrinsic Coercive Force (Hci): 1910 kA/m (24.0 kOe)	692832-3EA
Neodymium-iron-boron, alloy 30/100	Aluminum 0.8 wt. % Boron 1.1 wt. % Dysprosium 3.6 wt. % Iron 65 wt. % Neodymium 29 wt. % Niobium 0.5 wt. %	disc, 13 × 6 mm	Magnetic parameters/properties: Maximum Energy Product (BH): 239 kJ/m^3 (30 MGsOe) Residual Induction (Br): 1.14 T (11.4 kGs) Coercive Force (Hc): 820 kA/m (10.3 kOe) Intrinsic Coercive Force (Hci): 1114 kA/m (14.0 kOe)	693790-5EA
Neodymium-iron-boron alloy 30/150	Aluminum 0.8 wt. % Boron 1.1 wt. % Dysprosium 3.6 wt. % Iron 65 wt. % Neodymium 29 wt. % Niobium 0.5 wt. %	disc, 13 × 6 mm	Magnetic parameters/properties: Maximum Energy Product (BH): 247 kJ/m^3 (31 MGsOe) Residual Induction (Br): 1.13 T (11.3 kGs) Coercive Force (Hc): 844 kA/m (10.6 kOe) Intrinsic Coercive Force (Hci): 1595 kA/m (20.0 kOe)	693782-3EA
Neodymium-iron-boron, alloy 30/200	Aluminum 0.8 wt. % Boron 1.1 wt. % Dysprosium 3.6 wt. % Iron 65 wt. % Neodymium 29 wt. % Niobium 0.5 wt. %	disc, 13 × 6 mm	Magnetic parameters/properties: Maximum Energy Product (BH): 248 kJ/m^3 (31 MGsOe) Residual Induction (Br): 1.14 T (11.4 kGs) Coercive Force (Hc): 835 kA/m (10.5 kOe) Intrinsic Coercive Force (Hci): 2400 kA/m (30.0 kOe) Maximum Temperature rate: 200°C	693820-3EA

Hard Materials Center of Excellence

Materials and Services for High-tech Applications

The Aldrich® Center of Excellence for Hard Materials provides a range of products and custom services to suit the needs of both academic and industrial researchers. High-purity materials developed through the Center of Excellence address a wide variety of technology sectors from Alternative Energy and Advanced Electronics to Biomedical Applications. Materials expertise covers pure metals, alloys and metallurgical solids, salts, advanced ceramics, and complex oxides.

Capabilities include:

- Processing & purification of rare earth materials
- Forming & shaping of metals
- Purification of metals by vacuum distillation
- High temperature solid-state synthesis
- Beading of metals and metal salts
- High-purity salts
- Synthesis & packaging under controlled/inert-gas atmosphere
- Full analytical suite including XRD, particle size analysis, ICP-MS/OES, DSC/TGA, elemental analysis, and NMR

Examples of Recently Introduced Materials

Name	Formula	Purity (Trace Metals Basis)	Prod. No.
Antimony(III) telluride	Sb_2Te_3	99.99+%	740993
Barium tetrafluorocobaltate	$BaCoF_4$	99.9%	740969
Barium tetrafluoronickelate	$BaNiF_4$	99.9%	740918
Indium antimonide	InSb	99.99+%	740942
Scandium(III) oxide	Sc_2O_3	99.999%	294020
Tin(II) sulfide	SnS	99.99+%	741000

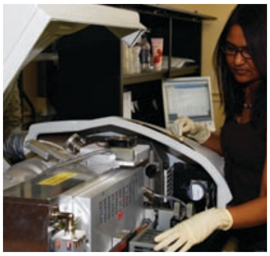

To inquire about our custom capabilities, contact us at **HardMaterials@sial.com**

Metal Hydrides for NiMH Battery Applications

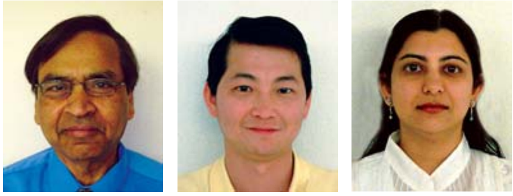

Dhanesh Chandra*, Wen-Ming Chien, and Anjali Talekar
University of Nevada, Reno, College of Engineering
Reno, NV 89557
*Email: dchandra@unr.edu

Introduction

Rechargeable solid-state batteries are becoming increasingly important due to wide-spread use in computers, portable electronics, and vehicular applications. The *Partnership for a New Generation of Vehicles (PNGV)*, a collaboration between the U.S. government and auto industry, was initiated in 1996 to promote the development of hybrid electric vehicles (HEVs) with significantly increased fuel economies. As shown in **Figure 1**, metal hydride and Li-ion batteries have high energy densities and are the most promising classes of modern rechargeable batteries.[1] Li-ion batteries are very attractive for modern portable electronic devices, and nickel metal hydride (NiMH) batteries are a significant component of modern hybrid automobiles. Based on 1996 prices, the estimated cost of these materials was <$1/gH produced (**Table 2**).[2-4] Although both NiMH and Li ion batteries are equally important for various applications, the cradle-to-gate (ctg) life E_{ctg}/kg basis is somewhat higher than that of other batteries (**Figure 2**).[5] This article is a summary of rare earth intermetallic compounds and their structures, properties, technologies, and applications, particularly with regard to rechargeable batteries.

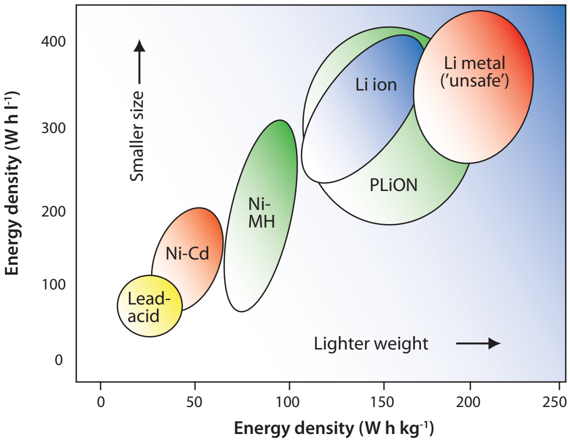

Figure 1. Comparison of volumetric and gravimetric energy density of the important NiMH, lead-acid (PbA), Ni-Cd, Na/S, and Li–ion batteries[1]

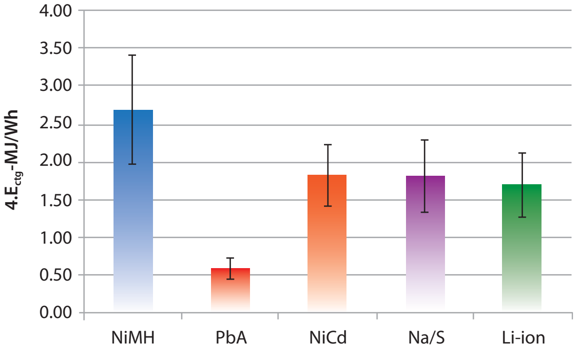

Figure 2. Average cradle-to-gate life (E_{ctg}) per watt hour basis with one standard deviation for NiMH, lead-acid (PbA), Ni-Cd, Na/S, and Li–ion batteries.[5]

Metal hydrides have been widely investigated over the years, with significant interest developing in the 1960s. The majority of research activities prior to 1960 are reported in *Metal Hydrides*, a book by Mueller, Blackledge, and Libowitz.[6] More recent work is covered in several good reviews by Schlapbach,[7] Sandrock,[8] Yvon,[9] Fukai,[10] Walker,[11] and others. In general, metastable binary or higher-order alloys that reversibly absorb/desorb hydrogen are preferred in applications due to their metastable nature: pure elements tend to form comparably stable hydrides. The precursor alloys that are used for hydrides are broadly classified into six categories based on A-B component systems.

Examples of simple binary systems, with no substitutions, are:

(1) AB (HfNi, FeTi)
(2) AB_2 (Mn_2Zn, $TiFe_2$)
(3) A_2B (Hf_2Fe, Mg_2Ni)
(4) A_2B_7 (Pr_2Ni_7, Ce_2Co_7)
(5) AB_3 ($NdCo_3$, $GdFe_3$)
(6) AB_5 ($LaNi_5$, $CeNi_5$)

The AB_5-type, $LaNi_5H_{6.7}$ hydrides have high volumetric capacities (~130 kgH_2/m^3), low gravimetric capacities (~2 wt.% H_2), and operate near room temperature. To help understand the development of these hydrides, the unsubstituted A-B hydrides will be discussed first in terms of hydrogen capacities. The following discussion will focus on the effect of one component substitution in the A-B systems. Finally, this article will address more practical hydrides, some of which are commercialized.

Thermodynamics and Crystal Structures of NiMH Battery Materials

Thermodynamics

Metal hydrides were first used for storage of hydrogen in the solid state. The alloys used for metal hydrides in NiMH battery applications are mainly AB_5- and AB_2-type; other alloy structures may be under consideration but will not be addressed here. **Table 1** describes some important properties of these model structure types.

Table 1. Intermetallic Compounds and their Hydrogen Storage Properties.[12]

Type of Hydride	Metal/ Alloy	Hydride	Structure	Wt.% Hydrogen	Peq., T(K)
Elemental	Pd	$PdH_{0.6}$	*Fm3m*	0.56	0.02 bar @ 298K
AB_5	$LaNi_5$	$LaNi_5H_6$	*P6/mm*	1.37	2 bar @ 298K
AB_2	ZrV_2	$ZrV_2H_{5.5}$	*Fd3m*	3.01	10^{-8} bar @ 323 K
A_2B	Mg_2Ni	Mg_2NiH_4	*P6mm*	3.59	1 bar @ 555 K
AB	FeTi	$FeTiH_2$	*Pm3m*	1.89	5 bar @ 303 K
BCC	TiV_2	TiV_2H_4	*BCC*	2.6	10 bar @ 313 K

The most important properties for battery applications are the hydrogen capacity, isotherm pressure, hysteresis, volumetric expansion/contraction, enthalpies, and hydriding/dehydriding temperatures. Additional properties are important for practical applications. These include the activation of alloys, decrepitation, kinetics, heat transfer, gaseous impurities in H_2, cyclic ability, safety, metallurgical fabrication of the alloys in large scale, cost, and recycling.

Thermodynamic properties are obtained by measuring volumetric isotherms using a Sieverts apparatus; these are now commercially available. Typically, we obtain isotherms at a constant temperature, yielding the H/M ratio and wt.% H. As the alloy starts to absorb hydrogen, a solid solution region is observed, called the α-phase. As more hydrogen is absorbed, the α→β phase transition occurs, giving the hydride phase in the plateau region. A schematic of this is shown in **Figure 3**; the x- and y-axes represent the hydrogen/metal ratio and pressure, respectively. Next, we measure many isotherms at different temperatures and obtain mid-plateau pressures. One generally observes hysteresis in the isotherms between desorption/absorption. Plotting ln P vs. 1/T(K) yields the van't Hoff plot, and the slope of the van't Hoff line gives ΔH/R. The enthalpy of formation is given by (-ΔH/R). The desired properties of the hydrides are estimated by creating a window of operation, *f(p,T)*. van't Hoff plots for many of the important hydrides are shown in **Figure 4**; these will be discussed later in the following sections. The α→β phase transition for AB_5 materials is described by the equations given below:

$$AB_5 + \frac{x}{2}H_2 \rightarrow AB_5H_x(\alpha - phase)$$

$$AB_5H_x(\alpha - phase) + \frac{x-7}{2}H_2 \rightarrow AB_5H_7(\beta - phase)$$

$$\Delta G_T^o = -RT\ln K_P$$

$$K_P = p_{H_2}(dehydriding), K_P = \left(p_{H_2}\right)^{-1}(hydriding)$$

$$\frac{\Delta H_T^o}{R} = -\frac{\partial \ln K_P}{\partial(1/T)} \; and \; \Delta S_T^o = -\frac{\Delta H_T^o - \Delta G_T^o}{T}$$

$$\ln p_{H2} = -\Delta H/RT + \Delta S/R$$

Here, M = metal or alloy (ex: $LaNi_5$), which first forms a solid solution phase with hydrogen, MH_y, designated as the α-phase. Then, this α-phase forms a hydride, MH_x. In the case of $LaNi_5$ (Aldrich Prod. No. 685933), the $LaNi_5$-H phase forms first and then the $LaNi_5H_7$ forms. There is only a solid solution region beyond a certain temperature ($T_{critical}$). The most important metal hydrides include several rare earth materials, which are listed in **Table 1**.[3,4]

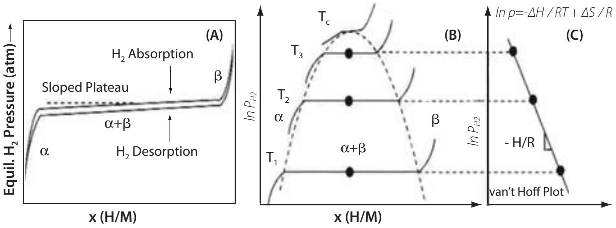

Figure 3. (A) An isotherm showing a sloped plateau for hydrogen absorption and desorption isotherms. Hysteresis between absorption and desorption isotherms is also shown. (B) The effect of temperature on the isotherm plateau pressure and phase transitions regions from α → α + β → β are shown. (C) The van't Hoff plot derived from the isotherms obtained at various temperatures; whose slope yields the enthalpy of hydriding.[18]

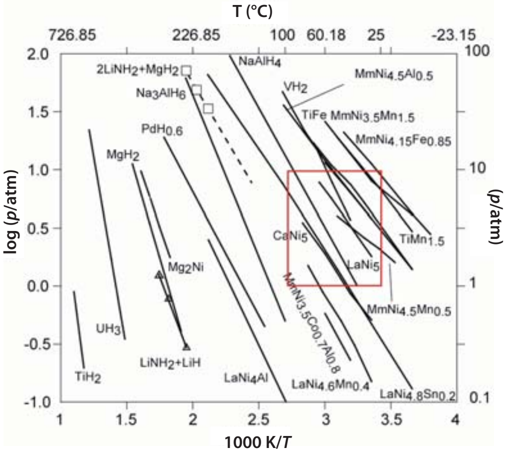

Figure 4. A compilation of the van't Hoff plots of selected elemental, classical, and complex hydrides. The boxed area represents the desired temperature and pressure range of operation for vehicular applications.[2,12,13,14,18]

As will be discussed later, there are many substituted compounds that effect thermodynamic properties. Some simple examples of cycling effects from our work on substituted $LaNi_5$ show significant disproportionation after 10,000 cycles (~1 h each) suggesting loss of hydriding properties (**Figure 5**). Simple Ni-site substitutions with small amounts of Sn improved cycle life significantly; even after 10,000 cycles there is no significant loss in hydrogen capacity in $LaNi_{4.8}Sn_{0.2}$ (**Figure 6**). Further details on thermal cycling and aging of substituted $LaNi_5$ alloys can be found in Lambert *et al.*,[15] Chandra *et al.*,[16] and Percheron-Guegan *et al.*[17] The knowledge of long-term cycling and thermal aging behavior of hydrides is essential to evaluate the hydrogen storage performance over a period of time. Thus, proper substitution of A or B in AB_5 or AB_2 can enhance cycle life, corrosion resistance properties, hysteresis, and electrochemical properties. Optimal stoichiometry battery alloys will be discussed in the following sections.

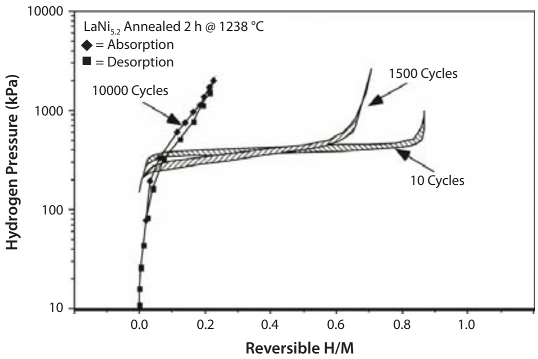

Figure 5. Isotherm of $LaNi_{5.2}$ taken at 25 °C after intrinsic P-T cycling for 10 (activation), 1500, and 10,000 times, showing severe degradation of this hydride.[15]

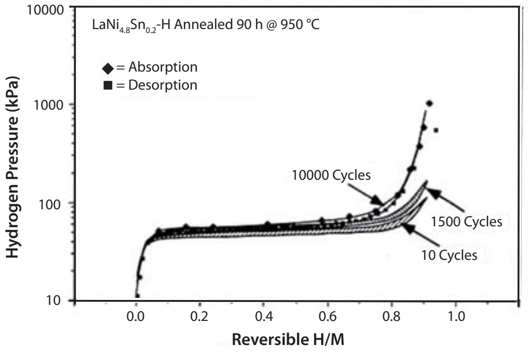

Figure 6. Isotherms of $LaNi_{0.8}Sn_{0.2}$ taken at 25 °C, before and after P-T intrinsic cycling for 1500 and 10,000 times showing virtually no loss in hydrogen capacity in the case of $LaNi_{0.8}Sn_{0.2}$.[15]

Crystal Structures of Battery Materials

Important properties for the MH battery are durability/cycle life, hydrogen capacity, and charge/discharge efficiency. From this standpoint, rare earth AB_5 and AB_2 metal hydrides are most desirable for long-range use in plug-in-hybrid-electric vehicle (PHEV) and electric vehicle (EV) applications. These are referred to as NiMH batteries and operate around ambient temperature. For example, the Toyota™ Prius (II-V models) use sealed NiMH batteries, which are estimated to have a 150,000 mile battery life based on the manufacturer's laboratory bench testing.[19] With further developments in the cycle life and energy densities of NiMH batteries, the upcoming electric vehicles may use these reliable high energy density batteries. These types of hydrides are now called "Classical Hydrides," but they have remarkable battery properties that are achieved by micro-alloying both A and B components, increasing the electrochemical and cycle life of the batteries.

Crystal Structure of AB_5 and AB_2 Hydride Materials

The crystal structures for the AB_5 and AB_2 compounds are listed in **Table 2**. The AB_5 compounds are line intermetallic compounds. AB_2 are intermetallic or intermediate compounds (with a small homogeneity range of compositions) and may not have the exact 1:2 stoichiometric composition.

Structure of AB_5 Compounds

Many NiMH batteries are made out of AB_5-type structure materials. The main base alloy materials are $LaNi_5$ and $MmNi_5$ (mischmetal-nickel alloy, Aldrich Prod. No. 685976), and the A and B components are invariably substituted in these materials to improve properties. The model compound, $LaNi_5$, has a hexagonal crystal structure, Strukturbericht $D2_d$ ($CaCu_5$-type, *P6/mmm*, $a = 5.0228$ Å, and $c = 3.9826$ Å). In the $LaNi_5$ structure, there is one site for La (1a site) and two different sites for Ni. The first Ni-site (2c site) is surrounded by La atoms and the other Ni-site (3g site) is located in the middle layer of the hexagonal structure with only Ni atoms. In many cases there is excess Ni (e.g., $LaNi_{5.2}$) and this varies the c/a ratio.[20] The structures of both the intermetallic $LaNi_5$ and the hydride are shown in **Figure 7**.[20-22]

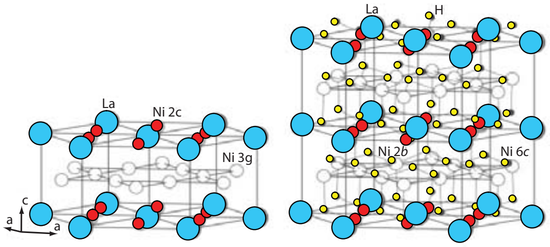

Figure 7. Crystal structure $LaNi_5$[20,21] and $LaNi_5H_7$.[22]

The hydride is $LaNi_5H_7$, which is generally ordered and is a line compound. Latriuge reported the structure to be a hexagonal double cell with a space group *P6₃mc*, $a = 5.409$ Å, and $c = 8.6$ Å.[21,22] Joubert *et al.*,[23] Thompson, Reilly and Hasting,[24] and many other groups have also reported this structure.

Practical battery materials are based on the AB_5 model. In one of the optimum commercial alloys, the A-site of $LaNi_5$ is substituted with mischmetal (Mm), which is a mixture of many elements ranging from atomic number 51 to 71. The B-site is substituted with Co-Al-Mn. Manufacturers of batteries have their variation of substitutions that are proprietary, but some promising alloys are listed in **Table 2** (Nos. 1 through 8). The alloy $MmNi_{3.5}Co_{0.7}Al_{0.8}$ (shown in **Figure 4** and **Table 2**) appears to be appropriate for battery properties and has the highest raw materials cost normalized to reversible capacity. Due to cost and other considerations, Co is not very desirable but is alloyed in small quantities for corrosion resistance.

Table 2. Selected classical hydrides with their hydrogen capacities and plateau pressures (Prices basis: mid-1996).[3,4,8]

No.	**Type**	**Selected Hydride**	**Temperature (K) @ 1 atm. p_{H2} (des.)**	**p_{H2} (des.) (atm.) @ 298K**	**Wt.% Hyd.**	**Density (g/cc)**	**ΔH° kJ/mol**	**ΔS° kJ/mol.K**	**Raw Materials Cost $/kg / $/gH**
1	AB_5	$MmNi_5$	217	23	1.46	8.6	21.1	0.097	7.94/0.64
2	AB_5	$MmNi_{4.1}5Fe_{0.85}$	241	11.2	1.14	8.1	25.3	0.105	7.12/0.79
3	AB_5	$MmNi_{4.5}Al_{0.5}$	267	3.8	1.20	8.1	28.0	0.105	7.17/0.79
4	AB_5	$LaNi_5$	285	1.8	1.49	8.3	30.8	0.18	9.87/0.77
5	AB_5	$LaNi_{4.8}Sn_{0.2}$	312	0.5	1.40	8.4	32.8	0.105	9.69/0.78
6	AB_5	$CaNi_5$	316	0.5	1.87	6.6	31.9	0.101	7.56/0.76
7	AB_5	$MmNi_{3.5}Co_{0.7}Al_{0.8}$	346	0.11	1.24	7.6	39.8	0.115	13.25/2.50
8	AB_5	$LaNi_{4.25}Al_{0.75}$	377	0.024	1.13	7.6	44.1	0.117	9.68/1.24
9	AB_2	$TiCr_{1.8}$	182	182	2.43	6	20.1	0.111	8.64/1.02
10	AB_2	$TiZr_{0.02}V_{0.43}Fe_{0.09}Cr_{0.05}Mn_{01.5}$	245	11	1.90	5.8	27.4	0.122	4.82/0.37
11	AB_2	$TiMn_{1.5}$	252	8.4	1.86	6.4	28.7	0.114	4.99/0.44
12	AB_2	$ZrFe_{1.5}Cr_{0.5}$	263	4	1.50	7.6	25.6	0.097	10.90/1.21
13	AB_2	$TiMn_{1.4}V_{0.62}$	268	3.6	2.15	5.8	28.6	0.016	29.40/2.67
14	AB_2	$ZrMn_2$	440	0.0001	1.77	7.4	53.2	0.121	11.29/1.25
15	A_2B	Mg_2NiH_4	528	0.00001	3.60	-	43.2	0.14	6.26/0.19
16	AB	TiFe	265	4.1	1.86	6.5	28.1	0.106	4.68/0.31
17	AB	$TiFe_{0.85}Mn_{0.15}$	276	2.6	1.90	6.5	29.5	0.107	4.83/0.32
18	AB	$TiFe_{0.8}Ni_{0.2}$	346	0.1	1.30	6.5	41.2	0.119	5.5/0.68
19	SS*	$(V_{0.9}Ti_{0.1})_{0.95}Fe_{0.05}$	309	0.5	3.70	6.0	43.2	0.140	10.63/0.59

Structure of AB_2 Compounds

Materials of the AB_2-type are generally Laves phase structures (Strukturbericht C14 and C15). This is another class of NiMH batteries; some important materials are listed in **Table 2** (Nos. 8 through 14). These materials also charge/discharge at near ambient temperatures like the AB_5 hydrides. The C14 materials may have cubic, orthorhombic, or hexagonal structures. **Figure 8** shows two types of common structures for C14 and C15 phases. An important example of C14 is $ZrMn_2$, which has a hexagonal structure with Z = 4 ($ZrMn_2$/formula unit) in the unit cell and is used for gas separation applications. The C15 structure of AB_2 has Z = 8/formula unit in the unit cell, as seen in ZrV_2-type materials; Yvon reported that H atoms occupy the A_2B_2 tetrahedral interstices.[27] Examples of AB_2 compounds include $GdMn_2$, HfV_2, $CeNi_2$, and $TiCr_{1.8}$.

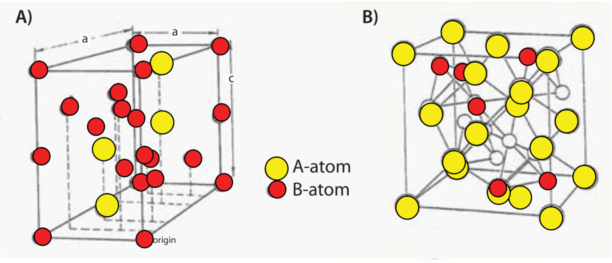

Figure 8. (A) One of the structures of the C14 Laves phases[25] and (B) one of the structures of the C15 Laves phases.[26]

In this AB_2 case, the common elements for A are Ti, Zr, Hf, and other rare earths (excluding Lu). Common B-site elements are Cr, V, Fe, and Mn. Many substitutions may be made for A and B to improve battery performance. Daimler Benz developed $TiZr_{0.02}V_{0.43}Fe_{0.09}Cr_{0.05}Mn_{01.5}$ (**Table 2**, No. 10, Aldrich Prod. No. 685941), a commercial alloy that has a reasonable price.[28]

The third class of materials that may have potential in NiMH batteries are AB hydrides. These generally have "CsCl"-type structures (Strukturbericht B2, space group Pm-3m). Libowitz[29] first reported ZrNi hydrides that hydrided around 100 °C, and in 1974, Reilly[30] developed an FeTi alloy (**Table 2**, No. 17) that formed FeTiH and $FeTiH_{1.5}$ and exhibited two plateaus at 30 °C. Reilly[31] also discovered $TiFe_{0.7}Mn_{0.2}$, which shows an H/M = 1 at 40 °C, and, Sandrock[32] developed $TiFe_{1-y}Al_y$ (y = 0.04 to 0.10), $TiFe_{0.85}Mn_{0.15}$, and $TiFe_{0.8}Ni_{0.2}$ (**Table 2**, Nos.17 and 18).[32]

Substitutions of A and B in AB_5 and AB_2 Compounds

The line compound hydrides are $LaNi_5$, YNi_5 (Aldrich Prod. No. 693928), $CeNi_5$, $MmNi_5$, and others. The A and B components are generally substituted to yield the most desirable properties. For example, the isotherm properties are modified to give a desirable plateau pressure, in some cases nearly two orders of magnitude near operating temperature. The $LaNi_5$ is a model compound that has a plateau pressure of 1.5 atm; $NdNi_5$, $CeNi_5$, and others also have high plateau pressures. A-site substitutions involve commercial mischmetal alloy mixtures (La, Pr, Ce, Nd). In this case hysteresis is increased but the hydrogen storage capacity is not reduced. Partial substitutions are also possible, in compounds such as $Mm_{1-x}CaNi_5$, which yield reduced plateau pressures as well as hysteresis. B-site substitutions of Ni with Pt, Cu, and others have not led to useful compounds. Partial substitution of the B-site, on the other hand, has led to many changes in thermodynamic properties. For battery applications, it is important that there is minimum volume change during hydriding/dehydriding; it was shown that addition of Co reduces volumetric change. Sakai reported that fully substituted $MmNi_5$, used in battery electrode applications, has some Co content to improve electrode life.[37] There are other patents and citations that have not been included in this review for brevity. The commercial B-substituted $MmNi_5$ alloys containing Co, Al, and Mn exhibit plateau pressures below 1 bar and good corrosion resistance. It is suggested that the commercial electrode alloy composition is approximately $MmNi_{3.5}Co_{0.8}Mn_{0.4}Al_{0.3}$. This alloy has great commercial value for battery applications as well as other hydrogen storage alloys for fuel cell and other stationary hydrogen storage applications. Partial B-site substitutions with Sn, Mn, In, and Si have also yielded superior performing hydrides. The most interesting ones that produced the optimum hydriding properties are Al and Sn. The well-known $LaNi_{4.5}Al_{0.5}$ has been used for Tritum applications. An example of single B-element substitution is shown for $LaNi_{5.2}$ and $LaNi_{4.8}Sn_{0.2}$ (**Figures 5** and **6**). It can be seen that thermal cycle life is profoundly affected by changes in alloying element. Bowman improved the properties of these alloys, which have been used for heat pumps in space applications.[33] In addition, it was found that cycle life improvements are possible with these substitutions.[34] Rare earths are also substituted in AB_2 compounds; compounds such as MmMnAl, LaMnAl, $TiZr_{0.02}V_{0.43}Fe_{0.09}Cr_{0.05}Mn_{01.5}$, and $TiMn_{1.4}V_{0.62}$ are equally important for our applications. Sandrock and Goodell also performed ambient pressure cycling on $Fe_{0.85}Mn_{0.15}Ti_{0.5}$ and showed the effect of gas impurities upon cycling.[35]

Electrochemical Reactions in NiMH Batteries

A schematic of a NiMH battery is shown in **Figure 9**, where the metal hydride is the negative electrode, NiO(OH)/$Ni(OH)_2$ is the positive electrode, and KOH is the electrolyte. On the positive side, the $Ni(OH)_2$ electrode oxidizes to NiO(OH) during charging and reduces back to $Ni(OH)_2$ during discharging. At the negative electrode, the metal hydride reduces to the alloy during discharge. The charge-discharge redox equations are also shown in **Figure 9**. It should be noted that there is no precipitation mechanism in this type of battery, as seen in Ni/Cd and others; the charge/discharge mechanism proceeds via proton transfer between Ni hydroxide and the metal hydride.

Over the years, these AB_5 compounds have been optimized for long cycle life, structural integrity, corrosion resistance, and low cost. It should be noted that substitution of AB_5 or AB_2 hydrides has a profound effect on the hydride properties, which have been optimized by battery manufacturers. The decrepitation of AB_5 electrodes was improved by addition of Co, Mn, and Al to $LaNi_5$ (Aldrich Prod. No. 685968). Koriyama reported the electrochemical durability of the electrodes due to substitution of various elements in $LaNi_5$ electrode, and these are listed in **Table 3**.[36]

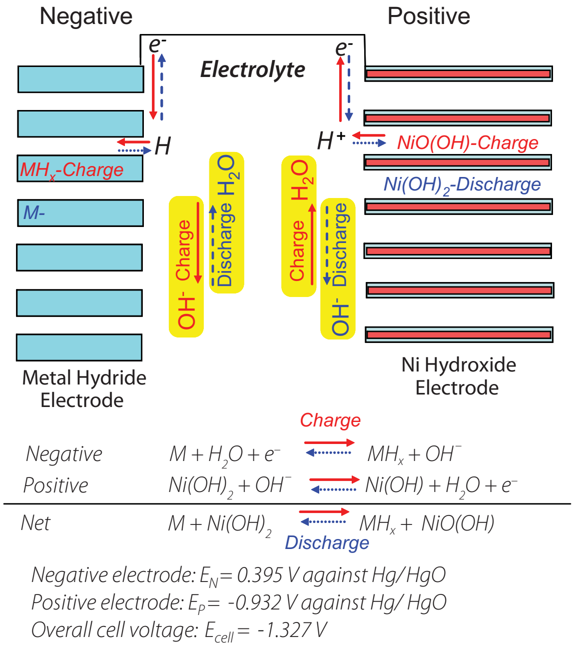

Figure 9. Charge-discharge mechanism in a NiMH battery.[36]

Typically, $Mm(Ni,Co,Mn,Al)_5$ powders or closely related compositions are used for batteries. The driving range for Mitsubishi® Libero EV has been established at 220 miles at 28 kwH battery storage energy based on 1999 report.[3] The cycle life of NiMH batteries is generally >1,000 with (practical) specific charge of 70-80 Wh/kg, although the theoretical charges are in the range of 220 and 230 Wh/kg for AB_5 and AB_2, respectively.[37] For the $MmNi_{3.6}Al_{0.4}Co_{0.7}Mn_{0.3}$ alloy, the discharge capacities of the alloy remain at 250 mAh/g with a nominal fading in capacity (to the extent of ~20 mAh/g) after prolonged cycling. Studies have also been performed on complex substituted alloys (from Sweden) of $MmNi_5$ [$(La_{0.58}Ce_{0.29}Nd_{0.08}Pr_{0.05})$ $(Ni_{3.6}Co_{0.7}Mn_{0.3}Al_{0.4})$] that showed improved activation and a high rate of discharge capacity by using sintered hydride electrodes.[38] Another example of cycle life of $LaNi_{4.7}Al_{0.0.3}$ as compared to $Mm_{0.95}Ti_{0.05}Co_{0.45}Mn_{0.35}Al_{0.15}$ is shown in **Figure 10**.[39] Another example of electrochemical cycling of $LaNi_{4.8}Sn_{0.1+x}$ showed that $LaNi_{4.8}Sn_{0.2}$ had better cyclic stability than the off-stoichiometric alloys such as $LaNi_{4.8}Sn_{0.1}$ and $LaNi_{4.8}Sn_{0.4}$ (**Figure 11**).

Table 3. Effects of substitution of La in $LaNi_5$-based alloy with other rare earths.[37]

Alloy	C(0), mAh•g^{-1}	C(100)/ C(0), %
$LaNi_5$	371	45
$LaNi_2Co_3$	292	90
$LaNi_2Co_{2.9}Al_{0.1}$	289	98
$LaNi_{3.55}Co_{0.75}Mn_{0.4}Al_{0.3}$	316	87
$La_{0.8}Ce_{0.2}Ni_{3.55}Co_{0.75}Mn_{0.4}Al_{0.3}$	327	93.6
$La_{0.5}Ce_{0.5}Ni_{3.55}Co_{0.75}Mn_{0.4}Al_{0.3}$	278	94.6
$Mm(1)Ni_{3.55}Co_{0.75}Mn_{0.4}Al_{0.3}$	283	92.2
$Mm(2)Ni_{3.55}Co_{0.75}Mn_{0.4}Al_{0.3}$	231	96.5

C(0): The capacity extrapolated to the 0th cycle, C(100): Capacity after 100 cycles.
Mm(1): Synthetic mishmetal [La:26%, Ce:52%, Nd:16%, Pr:6% (in atom%)]
Mm(2): Bastnasite (natural mishmetal) [La:18-28%, Ce:50-55%, Nd:12-18%, Pr:4-6%, and others: <2% (in atom%)]

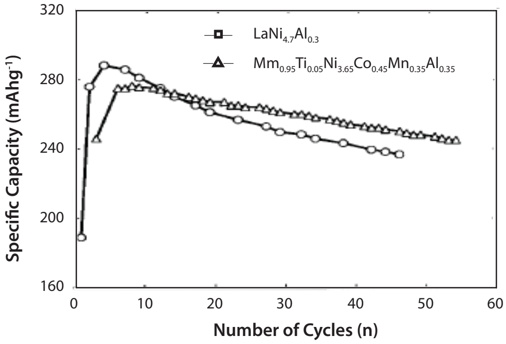

Figure 10. Discharge capacity of $Mm_{0.95}Ti_{0.05}Co_{0.45}Mn_{0.35}Al_{0.35}$ and $LaNi_{4.7}iAl_{0.3}$.[39]

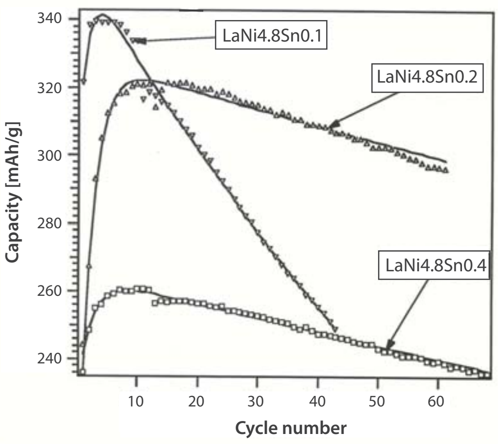

Figure 11. Discharge capacity of off-stoichiometric alloy, $LaNi_{4.8}iSn_{0.1+x}$.[40]

Societal Impacts of the Use of NiMH Batteries

NiMH hydride batteries are used in hybrid automobile batteries, electric razors, toothbrushes, cameras, camcorders, mobile phones, pagers, medical instruments/equipment, and numerous other applications. Because Li-ion battery technology is developing at an accelerated rate, development of NiMH battery materials must continue in order for this technology to remain competitive. NiMH batteries, however, appear to have slightly better life cycles than Li-ion batteries (**Figure 2**) on a MJ/Wh basis. It should be noted that the 2010 Toyota™ Prius uses Sanyo® Electric Co. NiMH batteries.

Metal hydrides have several other applications besides battery technology. Among them is hydrogen storage for vehicular fuel cell and internal combustion (IC) engine applications. These have great environmental implications, as the hydrogen vehicles emit water rather than CO_2. Many companies have made prototype hydrogen/fuel cell operated automobiles; Frank Lynch at HCI in Colorado developed metal tanks in the 1970s for the operation of Caterpillar® tractors using these hydrides. The main issue for practical modern automobiles is the development of reliable light-weight hydrides that are reversible and have approximately 10 wt.% H storage capacity. With additional development and optimization, it is hoped that some of the battery alloys listed in **Table 2** may someday be used for this purpose.

References

(1) Tarascon, J.-M.; Armond, M. *Nature* **2001**, *414*, 359.
(2) Sandrock, G.; Thomas, G. *IEA/DOE/SNL Hydride Database.* http://hydpark.ca.sandia.gov
(3) Sandrock, G.; Thomas, G. *Compilation of IEA/DOE/SNL databases* Technical Report for International Energy Agency (IEA): 1997.
(4) Reilly, J.; Wiswall, R.H., Jr. *Hydrogen Storage and Purification* Technical Report for Brookhaven National Laboratory: 1972.
(5) Sullivan, J.L.; Gaines, L. *A review of Battery Life-cycle Analyses: State of Knowledge and Critical Needs* Technical Report for Center for Transportation Research, Energy Systems Division, Argonne National Laboratory: 2010.
(6) Mueller, W.M.; Blackledge, J.P.; Libowitz, G.G. *Metal Hydrides*; Academic: New York, 1968.
(7) Schlapbach, L., Ed., *Hydrogen in Intermetallic Compounds I: Electronic, Thermodynamic, and Crystal lographic Properties, Preparation*; Springer: Berlin, 1988.
(8) Sandrock, G. *J. Alloys Compd.* **1999**, *293-295*, 877.
(9) Yvon, K. *Chimia*, **1998**, *52*, 613.
(10) Fukai, Y. *The Metal-Hydrogen System*; Springer-Verlag: Berlin, 1993.
(11) Walker, G. *Solid State Hydrogen Storage: Materials and Chemistry*; Woodhead Publishing: Cambridge, England, 2008.
(12) Sandrock, G. and Thomas, G. *Appl. Phys. A: Mater. Sci. Process.* **2001**, *72*, 153.
(13) Luo, W.; Ronnebro, E. *J. Alloys Compd.* **2005**, *404-406*, 392.
(14) Sandrock, G. Hydrogen Energy System: Production and Utilization of Hydrogen and Future Aspects. In *Application of Hydrides*; Yurum, Y., Ed.; Kluwer Academic: Dordrecht, 1995; p 135.
(15) Lambert, S.W.; Chandra, D.; Cathey, W.N.; Lynch, F.E.; Bowman, R.C., Jr. *J. Alloys Compd.* **1992**, *187*, 113.
(16) Chandra, D.; Bagchi, S.; Lambert, S.W.; Cathey, W.N.; Lynch, F.E.; Bowman, R.C., Jr. *J. Alloys Compd.* **1993**, *199*, 93.
(17) Percheron-Guegan, A.; Lartigue, C.; Archad, J.C. *J. Less-Common Met.* **1985**, *109*, 287.
(18) Chandra, D.; Reilly, J.J.; Chellappa, R. *JOM* **2006**, *58*, 26. http://www.springerlink.com/content/6302580987575252/
(19) Toyota Motor Corp. *Toyata Prius: Performance and Specifications.* http://www.Toyota.com/prius-hybrid/specs.html (accessed April 2011)
(20) Mizuno, M.; Araki, H.; Shirai, Y. *Int. J. Quantum Chem.* **2009**, *109*, 2758.
(21) Percheron-Guegan, A.; Lartigue, C. *Mater. Sci. Forum* **1988**, *31*, 125.
(22) Latroche, M.; Joubert, J.-M.; Percheron-Guegan, A; Bouree-Vigneron, F. *J. Solid State Chem.* **2004**, *177*, 1219.
(23) Joubert, J.-M.; Cerny, R.; Latroche, M.; Leroy, E.; Guenee, L., Percheron-Guegan, A.; Yvon, K. *J. Solid State Chem.* **2002**, *166*, 1.
(24) Thompson, P.; Reilly, J.J.; Hastings, J.M. *J. Less-Common Met.* **1987**, *129*, 105.
(25) Barrett, C.S. Crystal Structures of Metals. In *Metals Handbook, Vol. 8: Metallography, Structures, and Phase Diagrams*, 8th ed.; Lyman, T., Ed.; American Society for Metals: Metals Park, Ohio, 1973.
(26) Wernik, J.H. In *Intermetallic Compounds*; Westbrook, J.H., Ed.; John Wiley: New York, 1967; pp 197-216.
(27) Yvon, K.; Fisher, P. Crystal and Magnetic Structures of Ternary Metal Hydrides: A Comprehensive Review. In *Hydrogren in Intermetallic Compounds I: Electronic, Thermodynamic, and Crystallographic Properties, Preparation*; Schalpbach, L., Ed.; Springer: Berlin, 1988; pp 87-138.
(28) Benauer, O.; Zeigler, K. Hydrogen Storage Alloy. U.S. Patent 4,457,891, July 3, 1984.
(29) Libowitz, G.G.; Hays, H.F.; Gibbs, T.R.P *J. Phys. Chem.* **1958**, *62*, 76.
(30) Reilly, J.; Wiswall, R.H. *Inorg. Chem.* **1974**, *13*, 218.
(31) Reilly, J.J.; Johnson, J.R. *Proceedings of the World Hydrogen Energy Conference*, Coral Gables, Florida, 1976; Verziroglu, T.N., Ed.; Pergamon Press: New York, 1976; pp 8B-3 to 8B-26.
(32) Sandrock, G.D.; Reilly, J.J.; Johnson, J.R. *Proceedings of the 11th Intersociety Energy Conversion Engineering Conference*, State Line, Nevada, 1976; AICE: New York, 1976; pp 965-971.
(33) Bowman, R.C., Jr.; Luo, C.H.; Ahn, C.C. *J. Alloys Compd.* **1995**, *217*, 185.
(34) Goodel, P.D. *J. Less-Common Met.* **1984**, *99*, 1.
(35) Sandrock, G.D.; Goodell, P.D. *J. Less-Common Met.* **1980**, *73*, 161.
(36) Kuryama, N.; Miyamura, H.; Tnanka, H.; Ishikawa, H.; Uehara, I. *Vacuum* **1996**, *47*, 889.
(37) Sakai, T.; Uehera, I.; Ishikawa, H. *J. Alloys Compd.* **1999**, *293-295*, 762; Sakai, T.; Muta, K.; Miyamura, H.; Kuriyama, N.; Ishikawa, H. *Proceedings of the Symposium on Hydrogen Storage Materials, Batteries, and Electrochemistry*, Phoenix, Arizona, 1991; Corrigan, A. and Srinivasan S., Eds.; The Electrochemistry Society, 1992; Proc.Vol. 92-5, pp. 59-91.
(38) Geng, M.; Han, J.; Feng, F.; Northwood, D.O. *Int. J. Hydrogen Energy* **2000**, *25*, 203.
(39) Jiang, J.-J.; Gasik, M.; Laine, J.; Lampinen, M. *J. Alloys Compd.* **2001**, *322*, 281.
(40) Chandra, D.; Zuttel, A.; Chartouni, D.; Schlapbach, L. University of Freiburg. Unpublished work, 1996.

Rare Earth Metal Alloys for Hydrogen Storage and Battery Applications

For a complete list of available battery and hydrogen storage materials, visit Aldrich.com/energy

Name	Composition	Hydrogen Storage Capacity	Prod. No.
Lanthanum-nickel alloy	$LaNi_5$	1.5-1.6 wt.% @25°C	685933-10G
Lanthanum-nickel-cobalt alloy	$La_2Co_1Ni_9$	1.4-1.5 wt.% @25°C	685968-10G
Mischmetal-nickel alloy	$(Ce, La, Nd, Pr)Ni_5$	1.5-1.6 wt.% @25°C	685976-10G
Yttrium-Nickel alloy	YNi_5	-	693928-5G
Zirconium-scandium-iron alloy	$Zr_4Sc_1Fe_{10}$	-	693804-1G

Rare Earth Metals

For a complete list of available rare earth materials, visit Aldrich.com/periodic

Metal Powders

Name	Symbol	Purity	Physical Form	Prod. No.
Cerium	Ce	99.9% trace metals basis	powder	263001-10G
Erbium	Er	99.9% trace metals basis	powder	263044-5G
Gadolinium	Gd	99% trace metals basis	powder	263060-5G
Lanthanum	La	99.9% trace metals basis	powder	263109-25G
Lutetium	Lu	99.9% trace metals basis (Purity excludes ~2-3% Ta inherent in manufacturing process)	powder	263125-1G
Neodymium	Nd	≥99% trace metals basis	powder	460877-10G
Praseodymium	Pr	99.9% trace metals basis	powder	263176-5G
Samarium	Sm	99% trace metals basis	(powder or filings)	261203-1G 261203-10G 261203-50G
Samarium	Sm	-	powder	84433-10G 84433-50G
Scandium	Sc	99.9% trace metals basis	powder	261262-250MG 261262-1G
Thulium	Tm	99.9% trace metals basis	powder	263222-1G 263222-5G
Ytterbium	Yb	≥99.9% trace metals basis	powder	466069-2G
Ytterbium	Yb	99.9%	powder (under oil)	261297-2G 261297-10G
Yttrium	Y	99.9% trace metals basis	powder	261327-5G 261327-25G

Metal Foils

Name	Symbol	Purity	Prod. No.
Dysprosium	Dy	99.9%, metals basis (rare earth)	693707-1EA
Erbium	Er	99.9%, metals basis (rare earth)	693685-1EA
Gadolinium	Gd	99.9%, metals basis (rare earth)	693723-1EA
Holmium	Ho	99.9%, metals basis (rare earth)	693693-1EA
Lanthanum	La	99.9%, metals basis (rare earth)	694908-1EA
Lutetium	Lu	99.9%, metals basis (rare earth)	693650-1EA
Neodymium	Nd	99.9% (rare earth metals basis)	693758-1EA
Samarium	Sm	99.9%, metals basis (rare earth)	693731-1EA
Terbium	Tb	99.9% (rare earth metal basis)	693715-1EA
Thulium	Tm	99.9%, metals basis (rare earth)	693677-1EA
Ytterbium	Yb	99.9%, metals basis (rare earth)	693669-1EA
Yttrium	Y	99.9%, metals basis (rare earth)	693642-1EA

Bulk Metal Ingots and Chips

Name	Symbol	Purity	Physical Form	Prod. No.
Cerium	Ce	99.9% trace metals basis	chips chunks	461210-50G
Cerium	Ce	99.9% trace metals basis	ingot	261041-25G 261041-100G
Dysprosium	Dy	≥99.5%	pieces (small)	44640-5G
Dysprosium	Dy	99.9% trace metals basis	chips	263028-5G 263028-25G
Dysprosium	Dy	99.9% trace metals basis	ingot	261076-10G 261076-50G
Erbium	Er	99.9% trace metals basis	chips	263052-10G
Erbium	Er	99.9% trace metals basis	ingot	261084-10G
Europium	Eu	99.9% trace metals basis	chips in mineral oil	457965-5G
Europium	Eu	99.9% trace metals basis	ingot	261092-1G
Gadolinium	Gd	99.9% trace metals basis	chips	263087-10G 263087-50G
Gadolinium	Gd	99.99% (REM)	ingot	691771-10G
Gadolinium	Gd	99.9% trace metals basis	ingot	261114-10G
Holmium	Ho	99.9% trace metals basis	chips	457957-5G
Lanthanum	La	99.9% trace metals basis	ingot (under oil)	261130-25G
Lanthanum	La	99.9% trace metals basis	pieces	263117-25G
Lutetium	Lu	99.9% trace metals basis	ingot	261149-1G
Neodymium	Nd	99.9% trace metals basis	chips	263141-25G 263141-100G
Neodymium	Nd	99.9% trace metals basis	ingot	261157-25G
Praseodymium	Pr	99.9% trace metals basis	ingot	261173-10G 261173-50G
Samarium	Sm	99.9% trace metals basis	chips	261211-10G
Samarium	Sm	99.9% trace metals basis	ingot	263184-10G 263184-50G
Scandium	Sc	99.9% trace metals basis	dendritic pieces	261246-250MG 261246-1G
Terbium	Tb	99.9% trace metals basis	chips	263206-1G 263206-5G
Thulium	Tm	99.9% trace metals basis	chips	262978-1G
Ytterbium	Yb	99.9% trace metals basis	chips	262986-5G
Ytterbium	Yb	99.9% trace metals basis	chunks	548804-5G
Ytterbium	Yb	99.9% trace metals basis	ingot	261300-5G
Yttrium	Y	99.9% trace metals basis	chips	262994-5G
Yttrium	Y	99.9% trace metals basis	dendritic pieces	451347-1G 451347-5G
Yttrium	Y	99.9% trace metals basis	ingot	261319-10G 261319-50G

Rare Earth Oxides

For a complete list of available oxide materials, visit Aldrich.com/oxides

Bulk Metal Oxides

Name	Formula	Purity	Physical Form	Prod. No.
Cerium(IV) oxide	CeO_2	99.9% trace metals basis	fused pieces	342955-50G
Cerium(IV) oxide	CeO_2	99.995% trace metals basis	powder	202975-10G 202975-50G
Cerium(IV) oxide	CeO_2	99.9% trace metals basis	powder	211575-100G 211575-500G
Cerium(IV) oxide	CeO_2	90%	powder	348341-100G
Cerium(IV) oxide	CeO_2	≥99.0%	solid	22390-100G-F 22390-500G-F
Dysprosium(III) oxide	Dy_2O_3	≥99.99% trace metals basis	powder	203181-5G 203181-25G
Dysprosium(III) oxide	Dy_2O_3	99.9% trace metals basis	powder	289264-25G 289264-100G
Erbium(III) oxide	Er_2O_3	≥99.99% trace metals basis	powder	203238-5G 203238-25G
Erbium(III) oxide	Er_2O_3	99.9% trace metals basis	powder	289248-25G
Europium(III) oxide	Eu_2O_3	99.999% trace metals basis	powder and chunks	323543-1G 323543-5G
Europium(III) oxide	Eu_2O_3	99.99% trace metals basis	powder	203262-5G 203262-25G
Europium(III) oxide	Eu_2O_3	99.9% trace metals basis	powder	289221-5G 289221-25G
Gadolinium(III) oxide	Gd_2O_3	≥99.99% trace metals basis	powder	203297-5G
Gadolinium(III) oxide	Gd_2O_3	99.9% trace metals basis	powder	278513-25G 278513-100G
Holmium(III) oxide	Ho_2O_3	≥99.9% (rare earth content, expressed as Ho_2O_3)	powder	H9750-10G H9750-50G
Holmium(III) oxide	Ho_2O_3	99.999% trace metals basis	powder	229679-1G 229679-10G
Lanthanum(III) oxide	La_2O_3	99.999% trace metals basis	powder	203556-100G
Lanthanum(III) oxide	La_2O_3	99.99% trace metals basis	powder	199923-100G 199923-500G
Lanthanum(III) oxide	La_2O_3	≥99.9%	powder	L4000-100G L4000-250G L4000-500G L4000-1KG
Lanthanum(III) oxide	La_2O_3	≥99.9% trace metals basis	powder	289205-50G 289205-250G
Lanthanum(III) oxide	La_2O_3	99.98% (La)	solid	61550-100G-F 61550-500G-F
Lutetium (III) oxide	Lu_2O_3	99.99% trace metals basis	powder	203661-5G
Lutetium (III) oxide	Lu_2O_3	99.9% trace metals basis	powder	289191-5G
Neodymium(III) oxide	Nd_2O_3	99.99%	powder	203858-10G 203858-50G
Neodymium(III) oxide	Nd_2O_3	99.9% trace metals basis	powder	228656-25G 228656-100G
Praseodymium(III) oxide	Pr_2O_3	99.9% trace metals basis	powder	558249-10G
Praseodymium(III,IV) oxide	Pr_6O_{11}	99.999% trace metals basis	powder	204145-2G 204145-10G
Praseodymium(III,IV) oxide	Pr_6O_{11}	99.9% trace metals basis	powder	205176-50G 205176-250G
Samarium(III) oxide	Sm_2O_3	99.999% trace metals basis	powder	394394-5G 394394-25G
Samarium(III) oxide	Sm_2O_3	99.99% trace metals basis	powder	392537-25G
Samarium(III) oxide	Sm_2O_3	99.9% trace metals basis	powder	228672-10G 228672-100G
Scandium(III) oxide	Sc_2O_3	99.999% trace metals basis	powder	294020-500MG 294020-5G
Scandium(III) oxide	Sc_2O_3	99.9% trace metals basis	powder	307874-1G 307874-5G

Name	Formula	Purity	Physical Form	Prod. No.
Terbium(III) oxide	Tb_2O_3	99.99% trace metals basis	powder	590509-2G 590509-10G
Terbium(III,IV) oxide	Tb_4O_7	99.999% trace metals basis	powder	204579-2G
Terbium(III,IV) oxide	Tb_4O_7	99.9% trace metals basis	powder	253952-10G
Thulium(III) oxide	Tm_2O_3	99.99% trace metals basis	powder	204676-1G
Thulium(III) oxide	Tm_2O_3	99.9% trace metals basis	powder	289167-1G 289167-5G
Ytterbium(III) oxide	Yb_2O_3	99.99% trace metals basis	powder	204889-10G
Ytterbium(III) oxide	Yb_2O_3	99.9% trace metals basis	powder	246999-10G 246999-50G
Yttrium(III) oxide	Y_2O_3	99.999% trace metals basis	powder	204927-10G 204927-50G
Yttrium(III) oxide	Y_2O_3	99.99% trace metals basis	powder	205168-10G 205168-50G 205168-250G

Oxide Nanomaterials

Name	Formula	Description	Form	Prod. No.
Aluminum cerium oxide	$AlCeO_3$	99% trace metals basis, particle size <50 nm (BET)	nanopowder	637866-10G 637866-50G
Cerium(IV) oxide	CeO_2	particle size <25 nm (BET)	nanopowder	544841-5G 544841-25G
Cerium(IV) oxide	CeO_2	>99.95% trace metals basis, particle size <50 nm (BET)	nanopowder	700290-25G 700290-100G
Cerium(IV) oxide-calcium doped	-	particle size <100 nm	nanopowder	572403-25G
Cerium(IV) oxide, dispersion	CeO_2	avg. part. size 10 - 20 µm	dispersion	289744-100G 289744-500G
Cerium(IV) oxide, dispersion	CeO_2	particle size <25 nm	dispersion nanoparticles	643009-100ML 643009-250ML
Cerium(IV)-zirconium(IV) oxide	$(CeO_2)\cdot(ZrO_2)$	99.0% trace metals basis, particle size <50 nm (BET)	nanopowder	634174-25G 634174-100G
Dysprosium(III) oxide	Dy_2O_3	≥99.9% trace metals basis, particle size <100 nm (BET)	nanopowder	637289-25G
Dysprosium(III) oxide, dispersion	Dy_2O_3	≥99.9% trace metals basis, particle size <100 nm (BET) particle size <50 nm (XRD)	dispersion	639664-25ML
Erbium(III) oxide	Er_2O_3	≥99.9% trace metals basis, particle size <100 nm (BET)	nanopowder	637343-10G 637343-50G
Europium(III) oxide	Eu_2O_3	99.5% trace metals basis, particle size <150 nm (TEM)	nanopowder	634298-25G
Gadolinium(III) oxide	Gd_2O_3	99.8% trace metals basis, particle size <50 nm (XRD) particle size <100 nm (BET)	nanopowder	637335-10G 637335-50G
Holmium(III) oxide	Ho_2O_3	≥99.9% trace metals basis, particle size <100 nm (BET) particle size <50 nm (XRD)	nanopowder	637327-10G 637327-50G
Lanthanum(III) oxide	La_2O_3	99% trace metals basis, particle size <100 nm (TEM)	nanopowder	634271-25G
Neodymium(III) oxide	Nd_2O_3	99.9% trace metals basis, particle size <100 nm (BET)	nanopowder	634611-5G 634611-50G
Nickel(II) oxide	NiO	99.8% trace metals basis, particle size <50 nm (BET)	nanopowder	637130-25G 637130-100G 637130-250G
Samarium(III) oxide	Sm_2O_3	≥99% trace metals basis, particle size <100 nm (BET)	nanopowder	637319-10G
Terbium(III,IV) oxide	Tb_4O_7	99.5% trace metals basis, particle size <50 nm (XRD) particle size <100 nm (BET)	nanopowder	634255-25G
Ytterbium(III) oxide	Yb_2O_3	≥99.7% trace metals basis, particle size <100 nm (BET)	nanopowder	637300-10G
Yttrium(III) oxide	Y_2O_3	particle size <50 nm	nanopowder	544892-25G
Yttrium(III) oxide, dispersion	Y_2O_3	≥99.9% trace metals basis, particle size <100 nm (BET) particle size <50 nm (XRD)	nanoparticles	641901-100ML
Yttrium(III) oxide, dispersion	Y_2O_3	≥99.9% trace metals basis, <100 nm (DLS)	dispersion nanoparticles	702048-100G

ALDRICH
Materials Science

Solid Oxide Fuel Cell Materials

Fuel cells are battery-like systems that use hydrogen and oxygen to transform chemical energy into electricity. Similar to conventional batteries, fuel cells are composed of two electrodes (anode and cathode) and a conductive electrolyte. SOFCs are a distinct sub-class of fuel cell technology that operate at elevated temperatures (>773 K) and can potentially operate on carbon monoxide and hydrocarbons instead of solely hydrogen gas. Aldrich® Materials Science is pleased to offer a wide range of materials for use in SOFC applications.

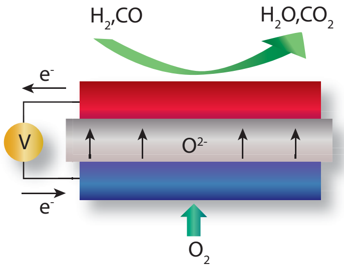

Solid Oxide Fuel Cell Electrolyte Materials

Name	Additives	Composition	Prod. No.
Cerium(IV) oxide, praseodymium doped	Praseodymium 20 mol% as dopant	$Ce_{0.8}Pr_{0.2}O_2$	729191
Cerium(IV) oxide-calcium doped	Calcium 10 mol% as dopant	$Ce_{0.9}Ca_{0.1}O_2$	572403
Cerium(IV) oxide-gadolinium doped	Gadolinium 20 mol% as dopant	$Ce_{0.8}Gd_{0.2}O_2$	572357
Cerium(IV) oxide-gadolinium doped	Gadolinium 10 mol% as dopant	$Ce_{0.9}Gd_{0.1}O_2$	572330
Cerium(IV) oxide-samaria doped	Samaria 15 mol% as dopant	$Ce_{0.85}Sm_{0.15}O_2$	572365
Cerium(IV) oxide-yttria doped	Yttria 15 mol% as dopant	$Ce_{0.85}Y_{0.15}O_2$	572381
Zirconium(IV) oxide-yttria stabilized	Yttria 0-10 mol% as stabilizer	$(ZrO_2)_{1-x}(Y_2O_3)_x$	544779
Zirconium(IV) oxide-yttria stabilized	Yttria 3 mol% as stabilizer	$(ZrO_2)_{0.97}(Y_2O_3)_{0.03}$	572322
Zirconium(IV) oxide-yttria stabilized	Yttria 8 mol% as stabilizer	$(ZrO_2)_{0.92}(Y_2O_3)_{0.08}$	572349
Zirconium(IV) oxide-yttria stabilized	Yttria ~8 mol% as stabilizer	$(ZrO_2)_{0.92}(Y_2O_3)_{0.08}$	464228
Zirconium(IV) oxide-yttria stabilized	Yttria ~5.3 mol% as stabilizer	$(ZrO_2)_{0.947}(Y_2O_3)_{0.053}$	464201

Solid Oxide Fuel Cell Electrode Materials

Name	Description	Composition	Prod. No.
Lanthanum nickelate, strontium doped		$La_{1.6}Sr_{0.4}NiO_4$	729183
Lanthanum nickelate		La_2NiO_4	729175
Lanthanum strontium cobalt ferrite, Cerium gadolinium oxide	LSCF/GDC composite cathode powder	$Ce_{0.9}Gd_{0.1}O_2$ 50 wt.%, $La_{0.6}Sr_{0.4}Co_{0.2}Fe_{0.8}O_3$ 50 wt.%	704253
Lanthanum strontium cobalt ferrite	LSCF 6428	$La_{0.6}Sr_{0.4}Co_{0.2}Fe_{0.8}O_3$	704288
Lanthanum strontium manganite	LSM-35	$La_{0.65}Sr_{0.35}MnO_3$	704261
Lanthanum strontium manganite	LSM-20	$La_{0.8}Sr_{0.2}MnO_3$	704296
Lanthanum strontium manganite, Cerium gadolinium oxide	LSM-20/GDC10 composite cathode powder	$Ce_{0.9}Gd_{0.1}O_2$ 50 wt.%, $La_{0.8}Sr_{0.2}MnO_3$ 50 wt.%	704237
Lanthanum strontium manganite	LSM-20/YSZ composite cathode powder	$(Y_2O_3)_{0.08}(ZrO_2)_{0.92}$ 50 wt.%, $La_{0.8}Sr_{0.2}MnO_3$ 50 wt.%	704245
Nickel oxide - Cerium samarium oxide	NiO/SDC for coatings	$(CeO_2\text{-}Sm_2O_3)$ 40 wt.%, NiO 60 wt.%	704210
Nickel oxide - Yttria-stabilized zirconia	NiO/YSZ general applications	NiO 60 wt.%, $Y_2O_3\text{-}ZrO_2$ 40 wt.%	704229
Nickel oxide - Yttria-stabilized zirconia	NiO/YSZ for coatings	$(Y_2O_3\text{-}ZrO_2)$ 34 wt.%, NiO 66 wt.%	704202

For detailed product information, view our technology spotlights at **Aldrich.com/sofc**

Sigma-Aldrich
3050 Spruce Street
St. Louis, MO 63103 USA

Sigma-Aldrich® Worldwide Offices

Argentina
Free Tel: 0810 888 7446
Tel: (+54) 11 4556 1472
Fax: (+54) 11 4552 1698

Australia
Free Tel: 1800 800 097
Free Fax: 1800 800 096
Tel: (+61) 2 9841 0555
Fax: (+61) 2 9841 0500

Austria
Tel: (+43) 1 605 81 10
Fax: (+43) 1 605 81 20

Belgium
Free Tel: 0800 14747
Free Fax: 0800 14745
Tel: (+32) 3 899 13 01
Fax: (+32) 3 899 13 11

Brazil
Free Tel: 0800 701 7425
Tel: (+55) 11 3732 3100
Fax: (+55) 11 5522 9895

Canada
Free Tel: 1800 565 1400
Free Fax: 1800 265 3858
Tel: (+1) 905 829 9500
Fax: (+1) 905 829 9292

Chile
Tel: (+56) 2 495 7395
Fax: (+56) 2 495 7396

People's Republic of China
Free Tel: 800 819 3336
Tel: (+86) 21 6141 5566
Fax: (+86) 21 6141 5567

Czech Republic
Tel: (+420) 246 003 200
Fax: (+420) 246 003 291

Denmark
Tel: (+45) 43 56 59 00
Fax: (+45) 43 56 59 05

Finland
Tel: (+358) 9 350 9250
Fax: (+358) 9 350 92555

France
Free Tel: 0800 211 408
Free Fax: 0800 031 052
Tel: (+33) 474 82 28 88
Fax: (+33) 474 95 68 08

Germany
Free Tel: 0800 51 55 000
Free Fax: 0800 64 90 000
Tel: (+49) 89 6513 0
Fax: (+49) 89 6513 1169

Hungary
Ingyenes telefonszám: 06 80 355 355
Ingyenes fax szám: 06 80 344 344
Tel: (+36) 1 235 9055
Fax: (+36) 1 269 6470

India
Telephone
Bangalore: (+91) 80 6621 9400
New Delhi: (+91) 11 4358 8000
Mumbai: (+91) 22 4087 2364
Hyderabad: (+91) 40 4015 5488
Kolkata: (+91) 33 4013 8000

Fax
Bangalore: (+91) 80 6621 9550
New Delhi: (+91) 11 4358 8001
Mumbai: (+91) 22 2579 7589
Hyderabad: (+91) 40 4015 5466
Kolkata: (+91) 33 4013 8016

Ireland
Free Tel: 1800 200 888
Free Fax: 1800 600 222
Tel: (+353) 402 20370
Fax: (+ 353) 402 20375

Israel
Free Tel: 1 800 70 2222
Tel: (+972) 8 948 4222
Fax: (+972) 8 948 4200

Italy
Free Tel: 800 827 018
Tel: (+39) 02 3341 7310
Fax: (+39) 02 3801 0737

Japan
Tel: (+81) 3 5796 7300
Fax: (+81) 3 5796 7315

Korea
Free Tel: (+82) 80 023 7111
Free Fax: (+82) 80 023 8111
Tel: (+82) 31 329 9000
Fax: (+82) 31 329 9090

Luxembourg
Tel: (+32) 3 899 1301
Fax: (+32) 3 899 1311

Malaysia
Tel: (+60) 3 5635 3321
Fax: (+60) 3 5635 4116

Mexico
Free Tel: 01 800 007 5300
Free Fax: 01 800 712 9920
Tel: (+52) 722 276 1600
Fax: (+52) 722 276 1601

The Netherlands
Free Tel: 0800 022 9088
Free Fax: 0800 022 9089
Tel: (+31) 78 620 5411
Fax: (+31) 78 620 5421

New Zealand
Free Tel: 0800 936 666
Free Fax: 0800 937 777
Tel: (+61) 2 9841 0555
Fax: (+61) 2 9841 0500

Norway
Tel: (+47) 23 17 60 00
Fax: (+47) 23 17 60 10

Poland
Tel: (+48) 61 829 01 00
Fax: (+48) 61 829 01 20

Portugal
Free Tel: 800 202 180
Free Fax: 800 202 178
Tel: (+351) 21 924 2555
Fax: (+351) 21 924 2610

Russia
Tel: (+7) 495 621 5828
Fax: (+7) 495 621 6037

Singapore
Tel: (+65) 6779 1200
Fax: (+65) 6779 1822

Slovakia
Tel: (+421) 255 571 562
Fax: (+421) 255 571 564

South Africa
Free Tel: 0800 1100 75
Free Fax: 0800 1100 79
Tel: (+27) 11 979 1188
Fax: (+27) 11 979 1119

Spain
Free Tel: 900 101 376
Free Fax: 900 102 028
Tel: (+34) 91 661 99 77
Fax: (+34) 91 661 96 42

Sweden
Tel: (+46) 8 742 4200
Fax: (+46) 8 742 4243

Switzerland
Free Tel: 0800 80 00 80
Free Fax: 0800 80 00 81
Tel: (+41) 81 755 2511
Fax: (+41) 81 756 5449

Taiwan
SAFC Hitech
Tel: (+886) 7 695 5066
Fax: (+886) 7 695 5088

Thailand
Tel: (+66) 2 126 8141
Fax: (+66) 2 126 8080

United Kingdom
Free Tel: 0800 717 181
Free Fax: 0800 378 785
Tel: (+44) 1747 833 000
Fax: (+44) 1747 833 313

United States
Toll-Free: 800 325 3010
Toll-Free Fax: 800 325 5052
Tel: (+1) 314 771 5765
Fax: (+1) 314 771 5757

Vietnam
Tel: (+84) 3516 2810
Fax: (+84) 6258 4238

Internet
sigma-aldrich.com

Green U Power

MIX
Paper from
responsible sources
FSC® C102832
FSC
www.fsc.org

Enabling Science to
Improve the Quality of Life

Order/Customer Service (800) 325-3010 • Fax (800) 325-5052
Technical Service (800) 325-5832 • sigma-aldrich.com/techservice
Development/Custom Manufacturing Inquiries SAFC® (800) 244-1173
Safety-related Information sigma-aldrich.com/safetycenter

World Headquarters
3050 Spruce St.
St. Louis, MO 63103
(314) 771-5765
sigma-aldrich.com

NOZ
76146-512100
1051

SIGMA-ALDRICH®